Comparative STM study of mixed ligand monolayers on gold nanoparticles in air and in 1-phenyloctane

Quy Khac Ong,[a] Shun Zhao,[a] Javier Reguera[a], Fabio Biscarini[b] and Francesco Stellacci[a]

[a] Institute of Materials, EPFL, Switzerland.
[b] Dip. Scienze della Vita, Università di Modena e Reggio Emilia, Via Campi 183, 41125 Modena, Italy.

Outline

1.1 Nanoparticles (NPs) synthesis

1.1.1 NP1: Octanethiol covered nanoparticles

1 mmol of chloro(triphenylphosphine)gold(I) was dissolved in 160 mL of benzene, 3 mmol of 1-octanethiol were added and left stirring for 10 min. After that 10 mmol of a borane *ter*t-butylamine complex dissolved in 160 mL of benzene were added to reduce the gold salt. The solution was heated immediately at 90 ºC and left to react for 60 min in strong stirring. After cooling the resulting solution was precipitated by the addition of methanol, and an extensive purification was performed by several cycles of centrifugation in acetone. ^{1}H NMR experiments were performed to verify the cleanness of nanoparticles.

1.1.2 NP2: nonanethiol:methylbenzenethiol covered nanoparticles

0.25 mmol of chloro(triphenylphosphine)gold(I) were dissolved in 20 mL of 1:1 toluene:tetrahydrofuran (THF), 0.5 mmol of ligands at the 1-nonanethiol:4-methylbenzenethiol (NT:MBT) 1:2 ratio were added and left stirring for 10 min. After that 2.5 mmol of a borane *ter*t-butylamine complex dissolved in 20 mL of toluene:THF 1:1 was added to reduce the gold salt. The solution was heated immediately at 80 ºC and left to react for 90 min in strong stirring. After cooling the resulting solution was precipitated by the addition of acetone, and an extensive purification was performed by several cycles of centrifugation in acetone. ^{1}H NMR experiments were performed to verify the cleanness of nanoparticles and the ligand ratio.

1.2 Characterization of gold nanoparticles

^{1}H NMR experiments were performed to verify the cleanness and to determine the ligand composition. NP size was determined by transmission electron microscopy (TEM, Fig. S2, ESI) and TGA was used to determine the ligand shell density (all results summarized in Table S1, ESI). The evaluation of the difference in ligand density between the two types of NPs will be done in future when more data will allow for an accurate estimation of the errors in TGA and NMR.

1.2.1 ^{1}H NMR experiments were performed in a Bruker AVIII-400 MHz. The purity of nanoparticles was evaluated by the absence of sharp peaks in the NMR spectra. In general, after the 4th or 5th cleaning, there was no significant change in the small sharp peaks, indicating a good cleanness of the nanoparticles. Once the nanoparticles were cleaned and dried, approximately ~ 5 mg of them were dissolved in 0.5 mL of $CDCl_3$ and 15 mg of iodine were added to etch the inorganic core. The NMR was performed directly on that solution after the etching was complete. The ligand ratio was obtained by comparing the terminal -CH_3 peaks of NT and MBT (~0.9 ppm and ~2.3 ppm respectively) (Figure S1, and table S1).

1.2.2 TEM images (Figure S2) were taken in a Philips/FEI CM12 operating at 100 kV. TEM grid preparation was done by drop-casting of dichloromethane solution of nanoparticles (0.1-0.5 mg /mL) onto a TEM grid standing on a filter paper to remove excess solvent. The images were analyzed using the Image J software package [http://rsbweb.nih.gov/ij/]. The default threshold was used and the diameter was calculated from the area assuming the particles were spherical. At least 1000 particles were counted on images of different areas of the grid to obtain significant statistics (Table S1).

1.2.3 Thermal gravimetric analysis (TGA) was performed on ~5 mg of these particles on a Perkin Elmer TGA 4000, temperature was ramped from 30 ºC to 800 ºC at a 10 ºC/min rate.

Table S1. Chemical and physical properties of the nanoparticles used in this study

Nanoparticle	Core diameter (nm)	Reaction ligand ratio (NT:MBT)	Ratio of Ligands found by ^{1}H NMR (NT:MBT)	Ligand density (ligands/ nm^2)
NP1	4.1 +/- 0.4	-	-	4.9
NP2	5.5 +/- 0.7	1:2	1: 1.3	5.8

1.3 STM samples preparation

Gold on mica substrates were purchased from Phasis (Switzerland). The fresh substrates were immersed in an ethanolic solution containing 1mM of 1-butanethiol. After 4 hours, the substrates were rinsed two times with ethanol and then immersed in a second solution containing 2 mM of 1-16-hexadecanedithiol for 24 hours to promote ligand exchange. The substrates were finally rinsed several times with ethanol, dried with a flow of nitrogen, and kept in a closed vial in argon atmosphere until their use.

Langmuir-Blodgett films were prepared in a KSV 2000 with a standard trough (150 mm width, 78000 mm^2) and symmetric barriers. 0.2 mL of ~1 mg/mL of NP $CHCl_3$ solution was deposited on the water subphase. After 10 min of the deposition, the barriers were closed at 10 mm/min. Once the solid phase was reached, the system was left to equilibrate, the nanoparticle monolayer was then transferred, in a parallel fashion (Langmuir-Schaefer deposition), onto the functionalized Au(111)-coated mica substrates.

1.4 UV-Visible spectroscopy

UV-Visible spectroscopy was performed in a Lambda 25 (Perking Elmer). A small quantity of each sample was dissolved in 1-phenyloctane and sonicated for 2 min. The solution was left to equilibrate for one hour and measured after that. The UV-Vis spectra (Figure S3) show that 1-phenyloctane is a good solvent for **NP1** but for the case of **NP2** there is only a partial solubility.

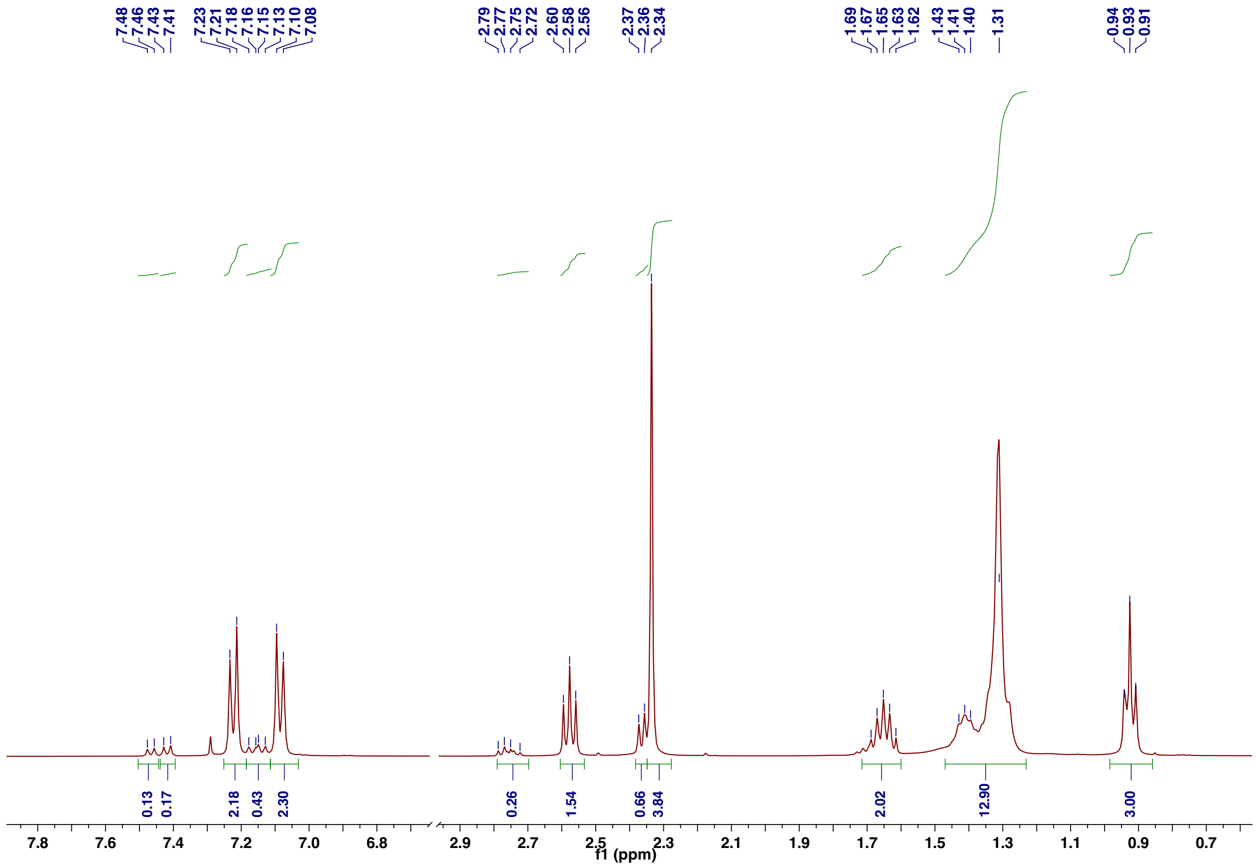

Figure S1. ^{1}H NMR spectra of the **NP2** in $CDCl_3$ solvent after iodine etching.

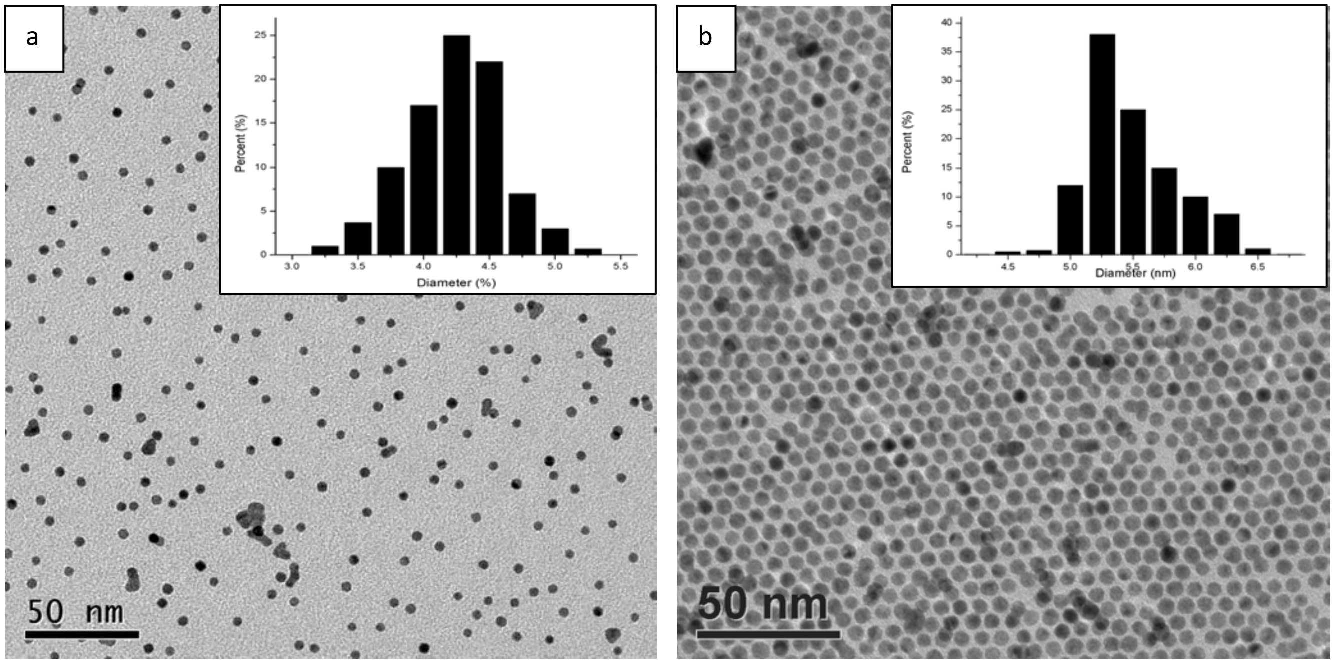

Figure S2. TEM image of gold nanoparticles: (a) **NP1**, and (b) **NP2**. Insets show the histogram of the size distribution for the particles. Scale bars are 50 nm.

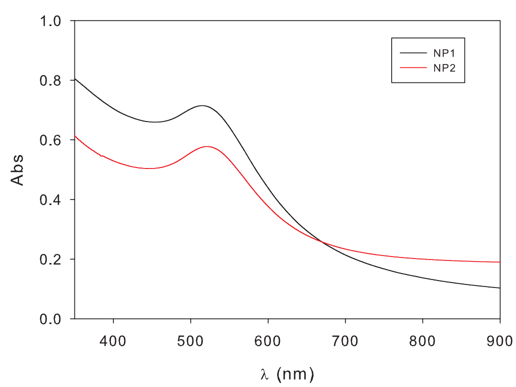

Figure S3: UV-Vis spectra of **NP1** and **NP2** in 1-phenyloctane. The wavelength of the surface plasmon resonance is 515 and 520 nm respectively. The redshift for **NP2** together with the lower decrease of the absorbance at higher wavelengths is indicative of formation of aggregates due to the decrease in solubility.

2. Additional STM images

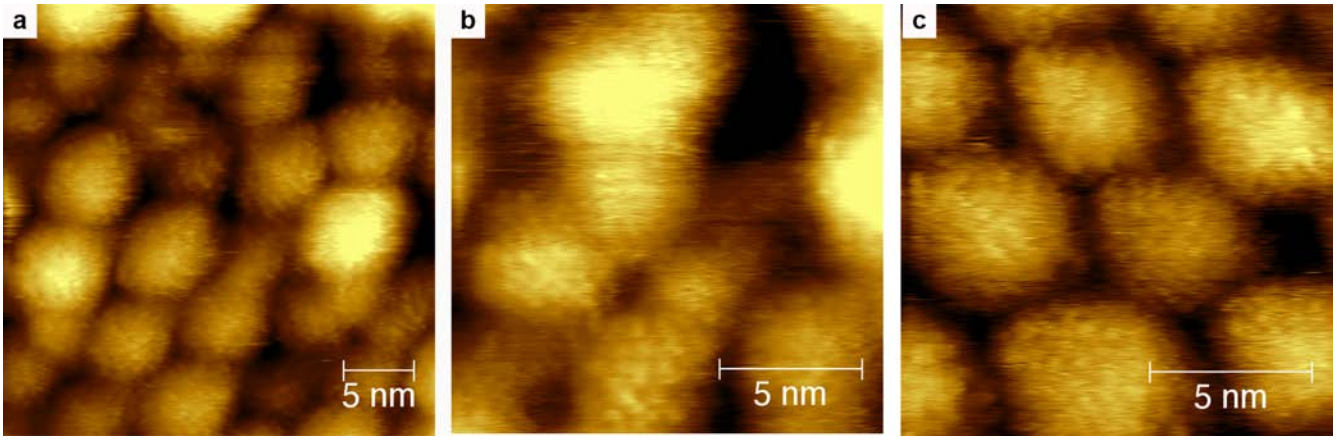

Figure S4. STM topography images of **NP2** in air. a) Image recorded with Vb = +500 mV, It = 50 pA, Ss = 30x30 nm^2, Vt= 1.22 µm/s, Pi =0.41. b) Image recorded with Vb = +500 mV, It = 50 pA, Ss = 15x15 nm^2, Vt= 0.91 µm/s, Pi =0.41. c) Image recorded with Vb = +800 mV, It = 200 pA, Ss = 13.2x13.2 nm^2, Vt= 0.73 µm/s, Pi =0.45.

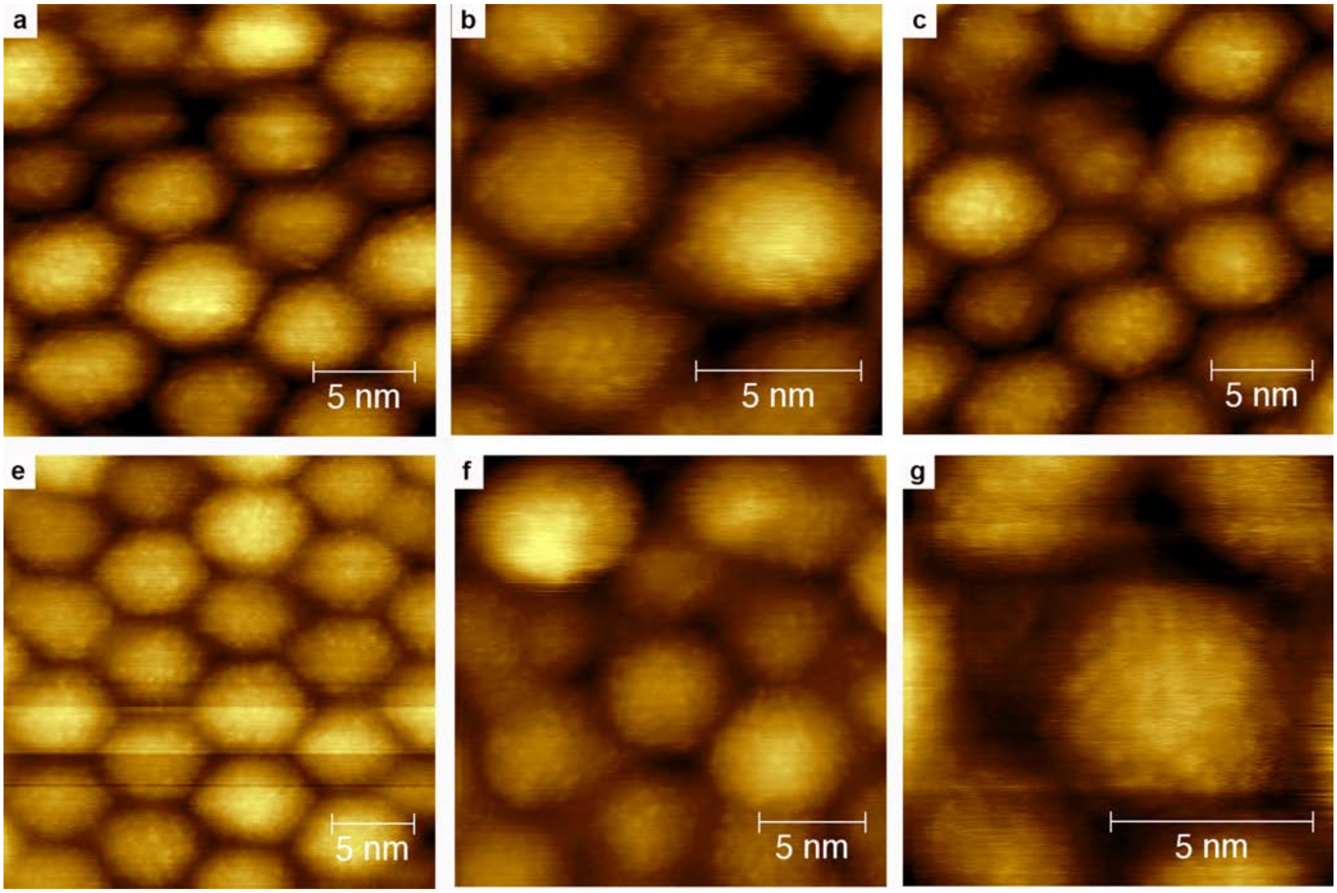

Figure S5. STM topography images of **NP1** in air. a) Image recorded with Vb = +700 mV, It = 50 pA, Ss = 12.9x12.9 nm^2, Vt= 0.79 µm/s, Pi =0.45. b) Image recorded with Vb = +700 mV, It = 50 pA, Ss = 21x21 nm^2, Vt= 0.64 µm/s, Pi =0.45. c) Image recorded with Vb = +700 mV, It = 50 pA, Ss = 21x21 nm^2, Vt= 0.85 µm/s, Pi =0.5. e) Image recorded with Vb = +700 mV, It = 50 pA, Ss = 25.8x25.8 nm^2, Vt= 0.79 µm/s, Pi =0.45. f) Image recorded with Vb = +800 mV, It = 50 pA, Ss = 20x20 nm^2, Vt= 0.81 µm/s, Pi =0.45. g) Image recorded with Vb = +800 mV, It = 50 pA, Ss = 10.5x10.5 nm2, Vt= 0.64 µm/s, Pi =0.45.

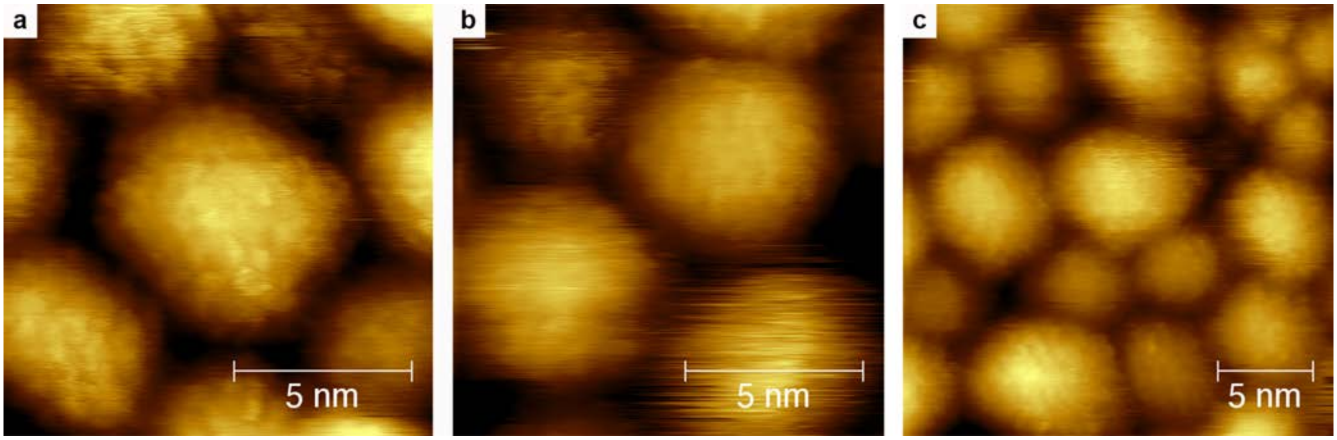

Figure S6. STM topography images of **NP2** in PO. a) Image recorded with Vb = +500 mV, It = 50 pA, Ss = 12x12 nm^2, Vt= 0.73 µm/s, Pi =0.43. b) Image recorded with Vb = +500 mV, It = 50 pA, Ss = 12x12 nm^2, Vt= 0.73 µm/s, Pi =0.43. c) Image recorded with Vb = +500 mV, It = 50 pA, Ss = 22.3x22.3 nm^2, Vt= 0.91 µm/s, Pi =0.43.

3. STM control

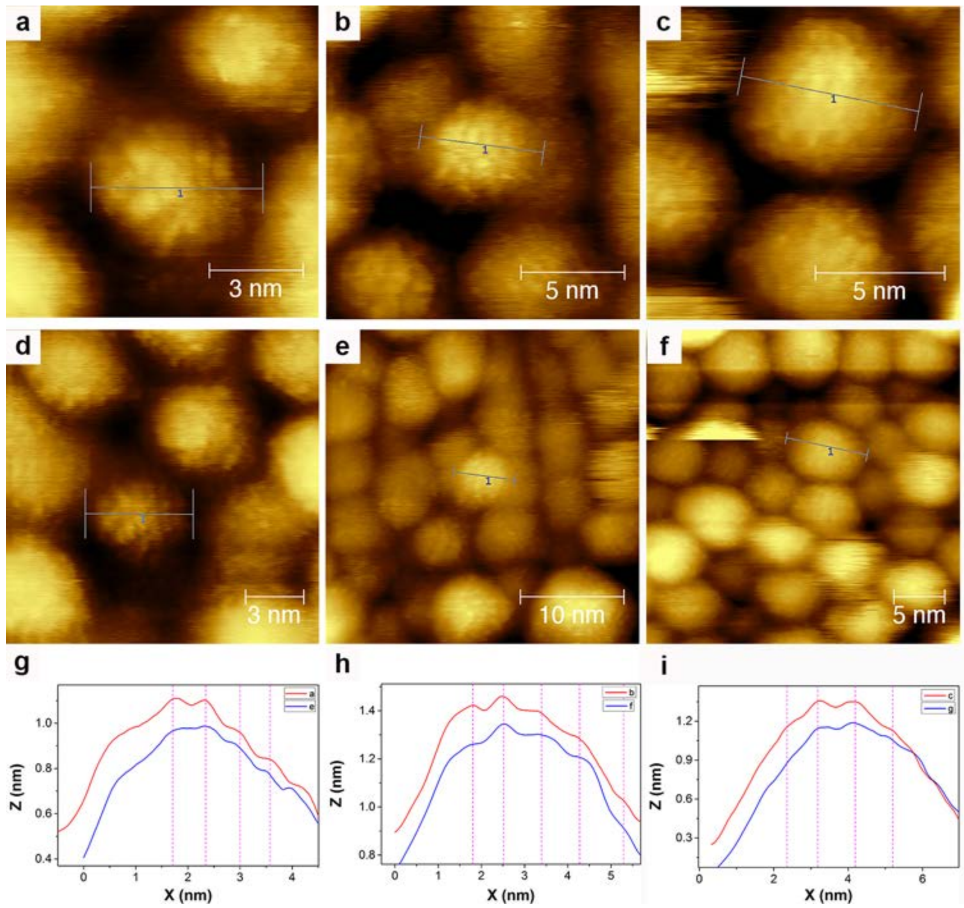

Figure S7. STM topography images of NP1 in air (a,d) NP2 in air (b, e) and NP2 in PO (c, f). The bright "scar" in Fig. 2f was caused by a particle sitting unstably on the array of particles underneath, and therefore being swept away by the STM tip. All images are the full trace scan. The bottom row (g,h,i) shows cross sectional profiles of the same particle imaged at two different magnifications displayed in the column above.

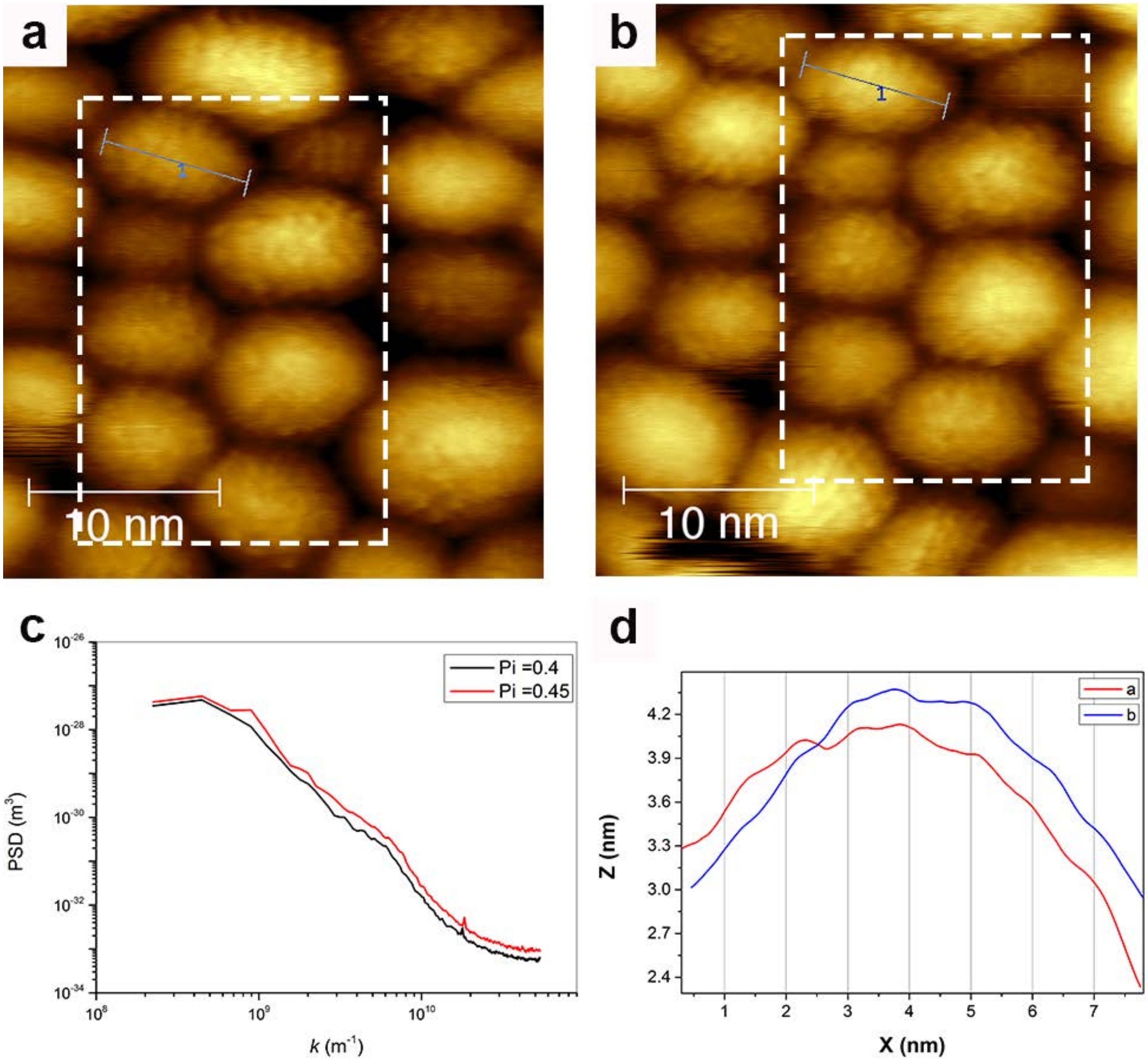

Figure S8. STM images of striped NPs remain consistent with respect to the integral gain. (a) Pi = 0.40, (b) Pi = 0.45, (c) the overlap of PSD curves from image a and b. d) cross-section profiles (marked by number 1 in the images) of the same particles present in both image a and b showing the consistency of stripe width versus gain change. Both images were recorded with Vb = +600 mV, It = 40 pA, Ss = 30x30 nm^2, Vt= 1.22 μm/s.

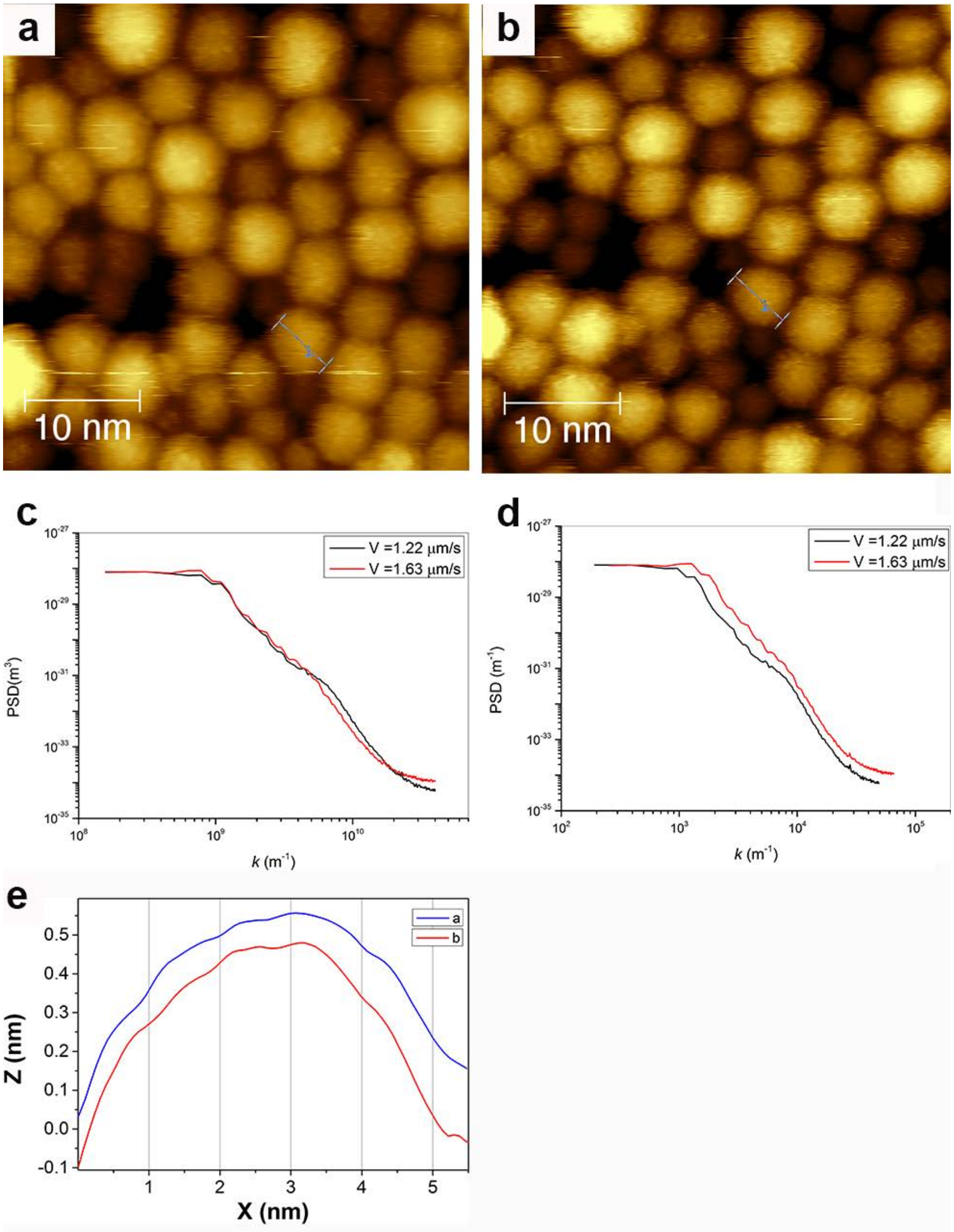

Figure S9. STM images of **NP2** in air remain consistent with respect to tip velocity. (a) Vt = 1.22 μm/s, (b) Vt = 1.62 μm/s, (c) the overlap of PSD curves from image a and b in spatial frequency space, (d) the shift of PSD curves from image a and b in time frequency space. (e) cross-section profiles (marked by number 1 in the images) of the same particle in image a and b showing the consistency of their stripe width. Both images were recorded with Vb = +800 mV, It = 200 pA, Ss = 40x40 nm^2, Pi = 0.45.

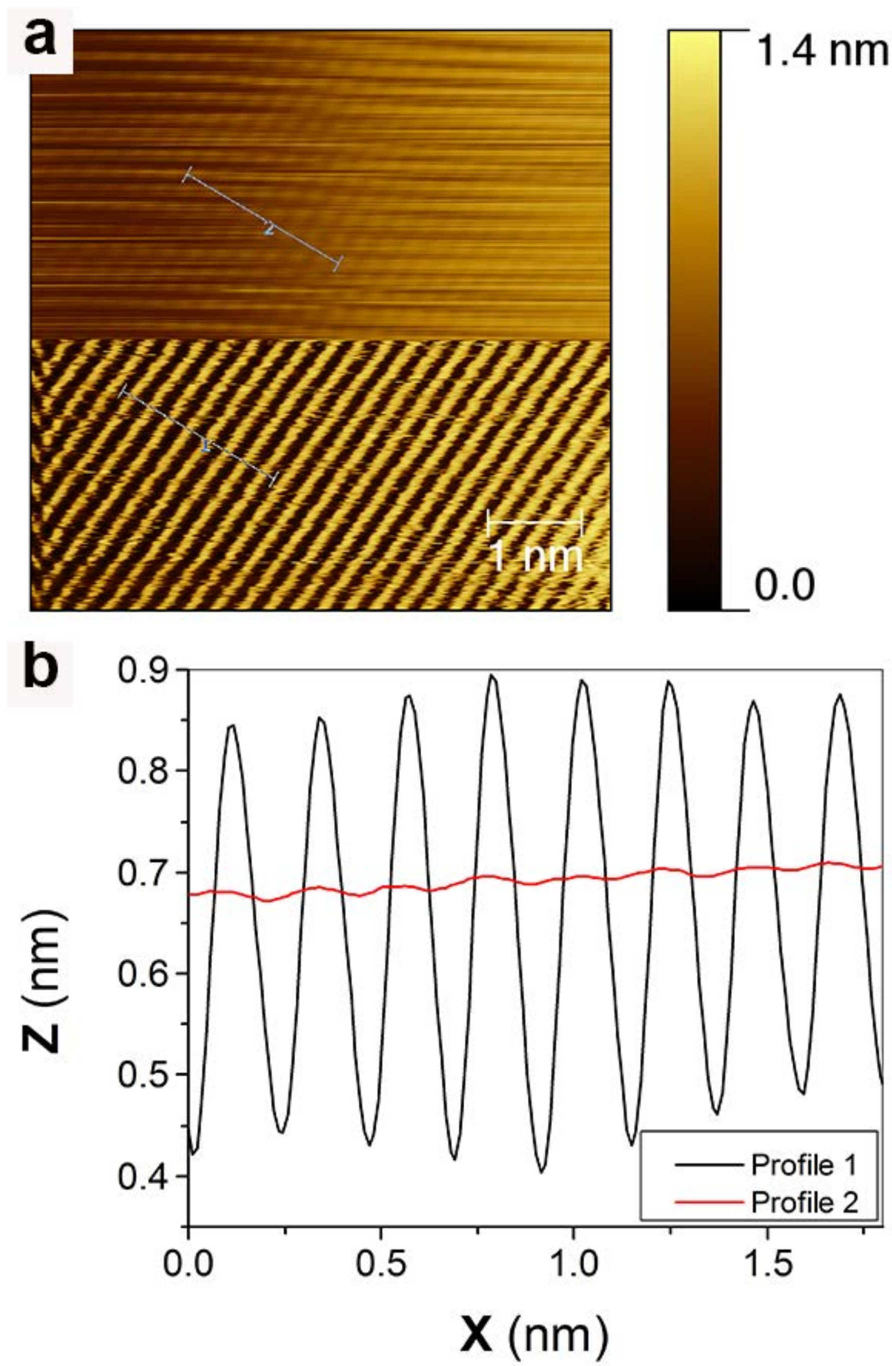

Figure S10. STM image and cross section analysis of an HOPG surface recorded as the integral gain (Pi) was suddenly changed from Pi =0.2 (upper half) to Pi =10 (lower half) in the middle of the image while keeping all other imaging parameters constant. Image recorded with Vb = +100 mV, It = 1000 pA, Ss = 6x6 nm^2, Vt= 0.24 μm/s. b) cross section analysis of indicated lines in the image a.

4. PSD curves and fitting

PSD spectra were calculated by free open-source software Gwyddion. [1]

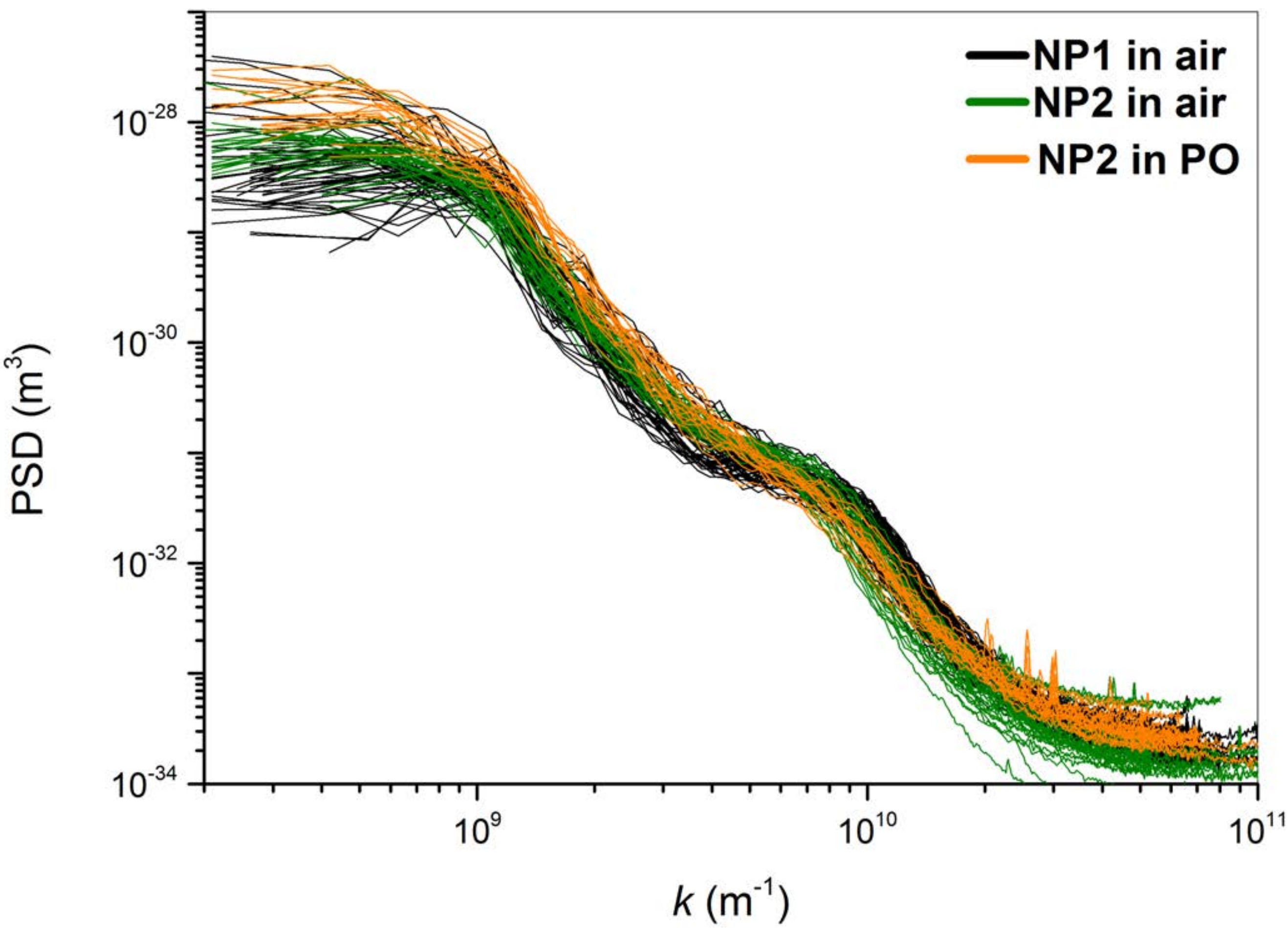

Figure S11. All PSD curves of all the particles in this study.

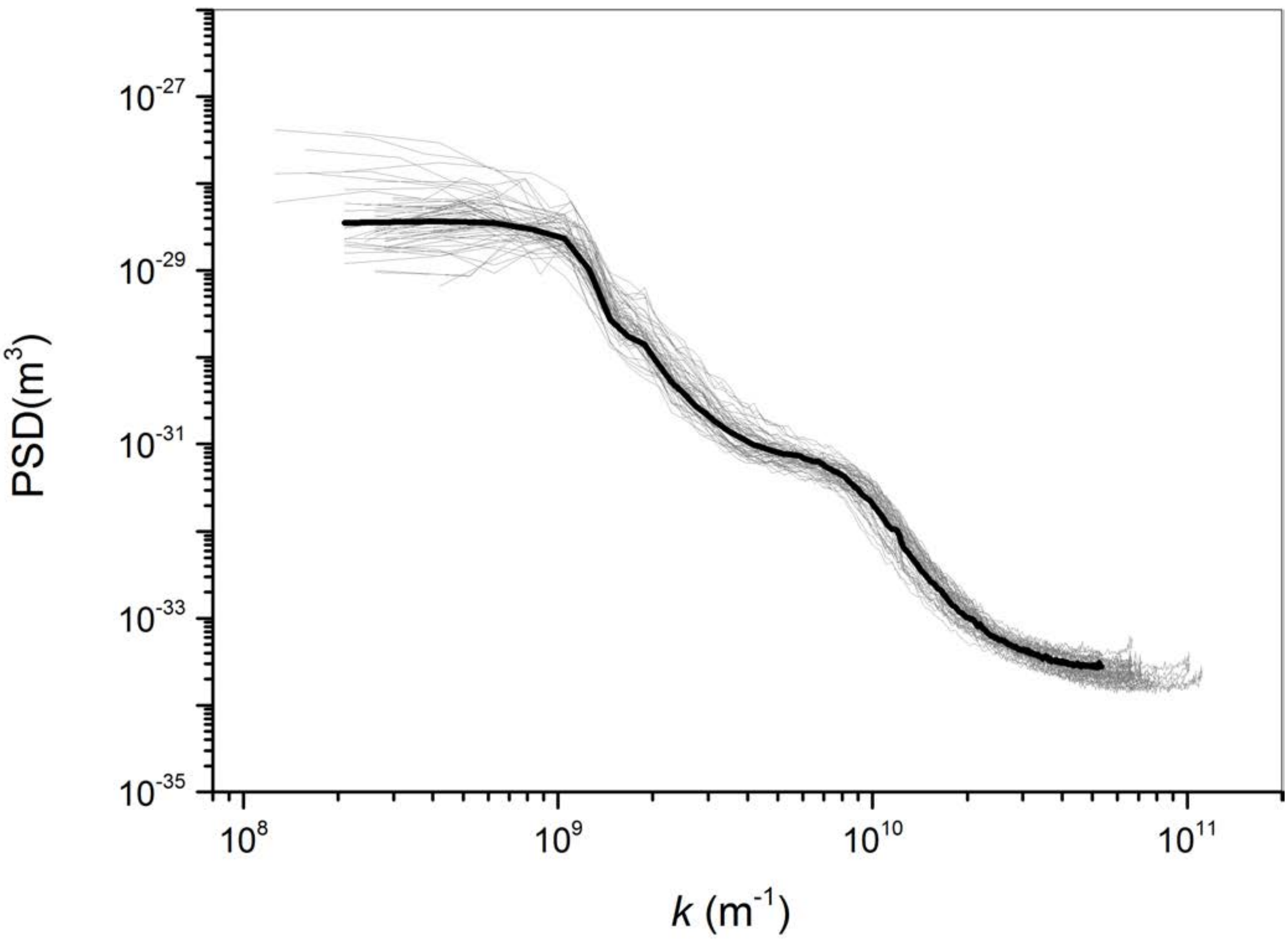

Figure S12. All PSD curves (light gray) and the average PSD curve (black) of **NP1** images recorded in air.

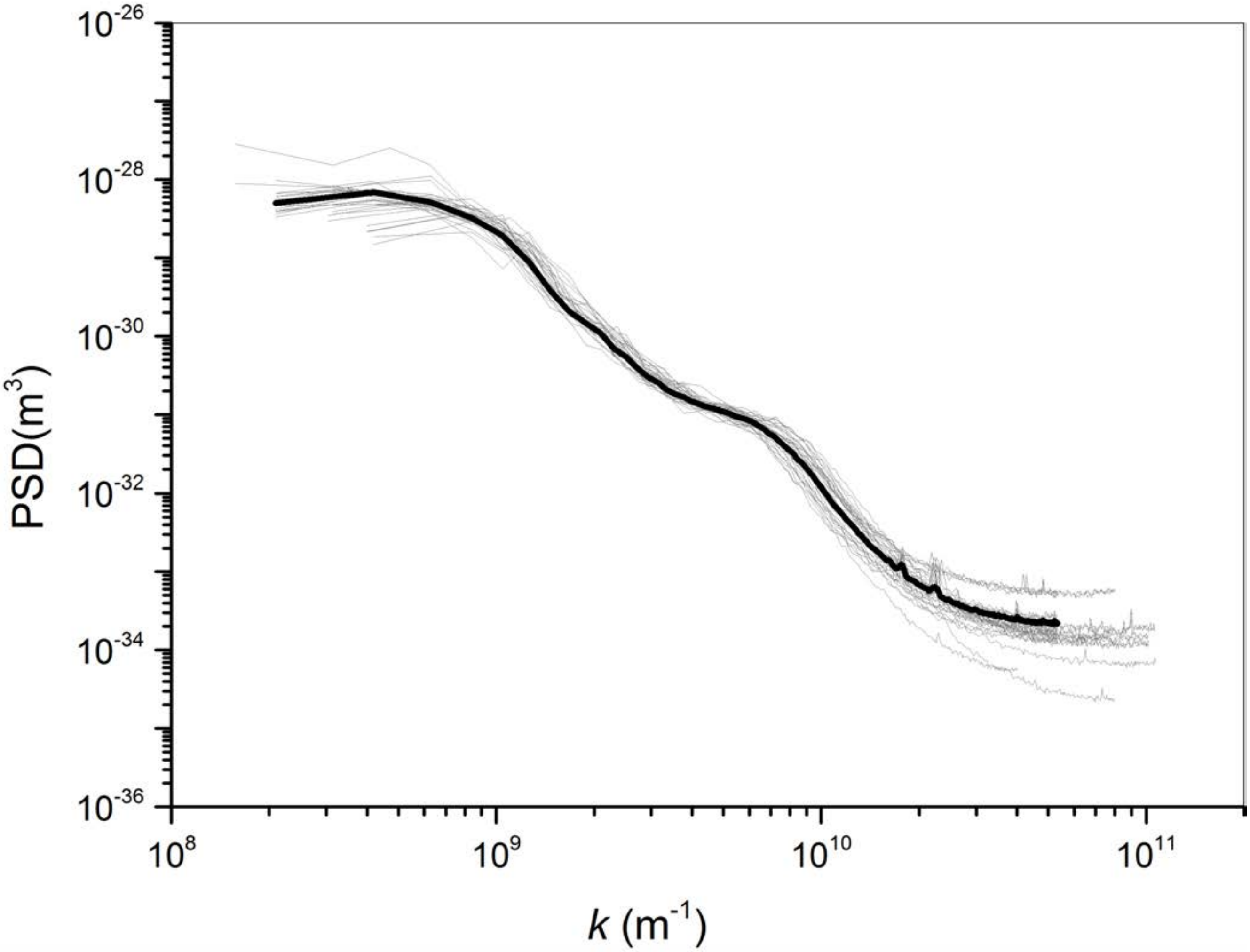

Figure S13. All PSD curves (light gray) and the average PSD curve (black) of **NP2** images recorded in air.

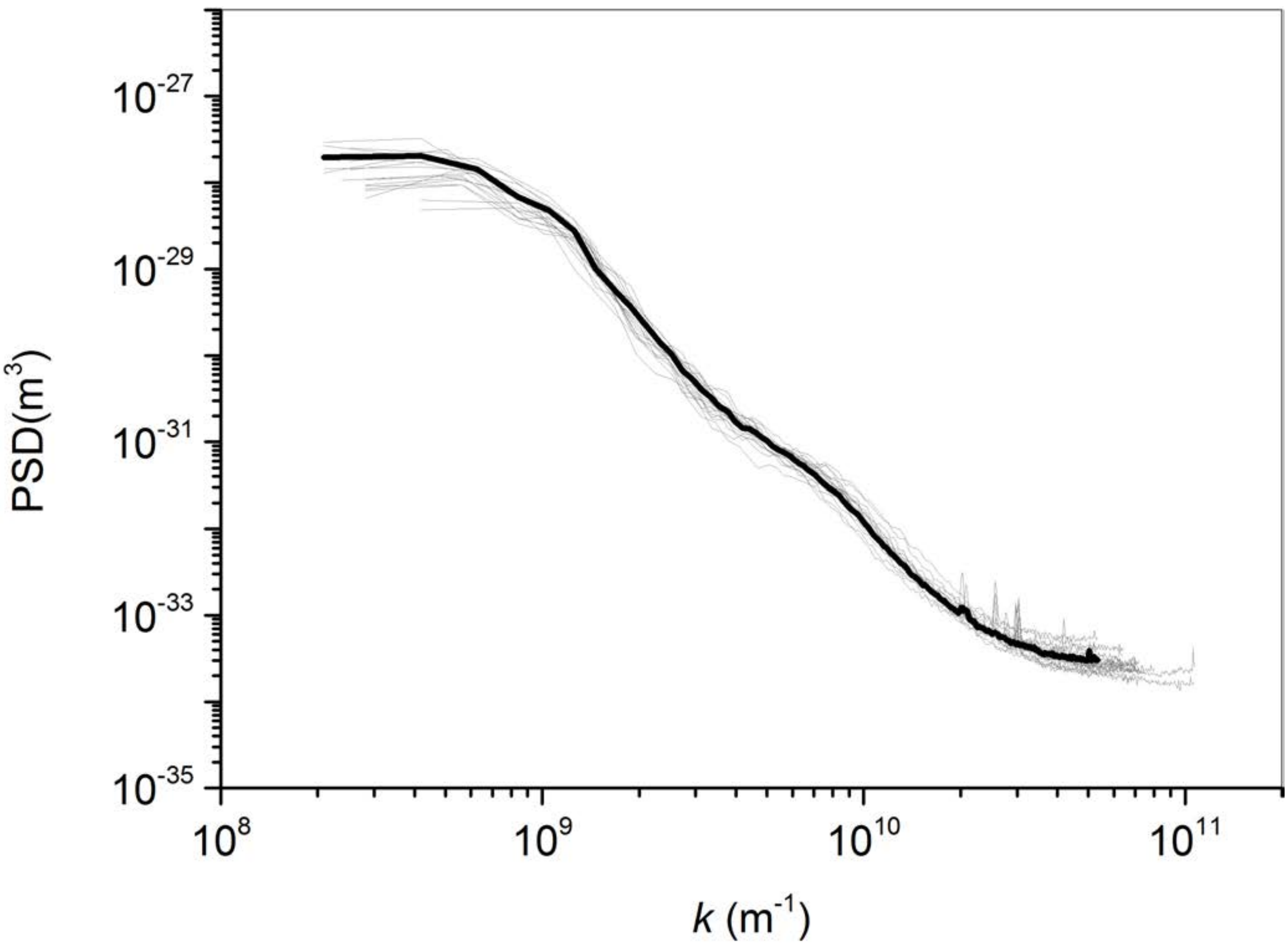

Figure S14. All PSD curves (light gray) and the average PSD curve (black) of **NP2** images recorded in PO.

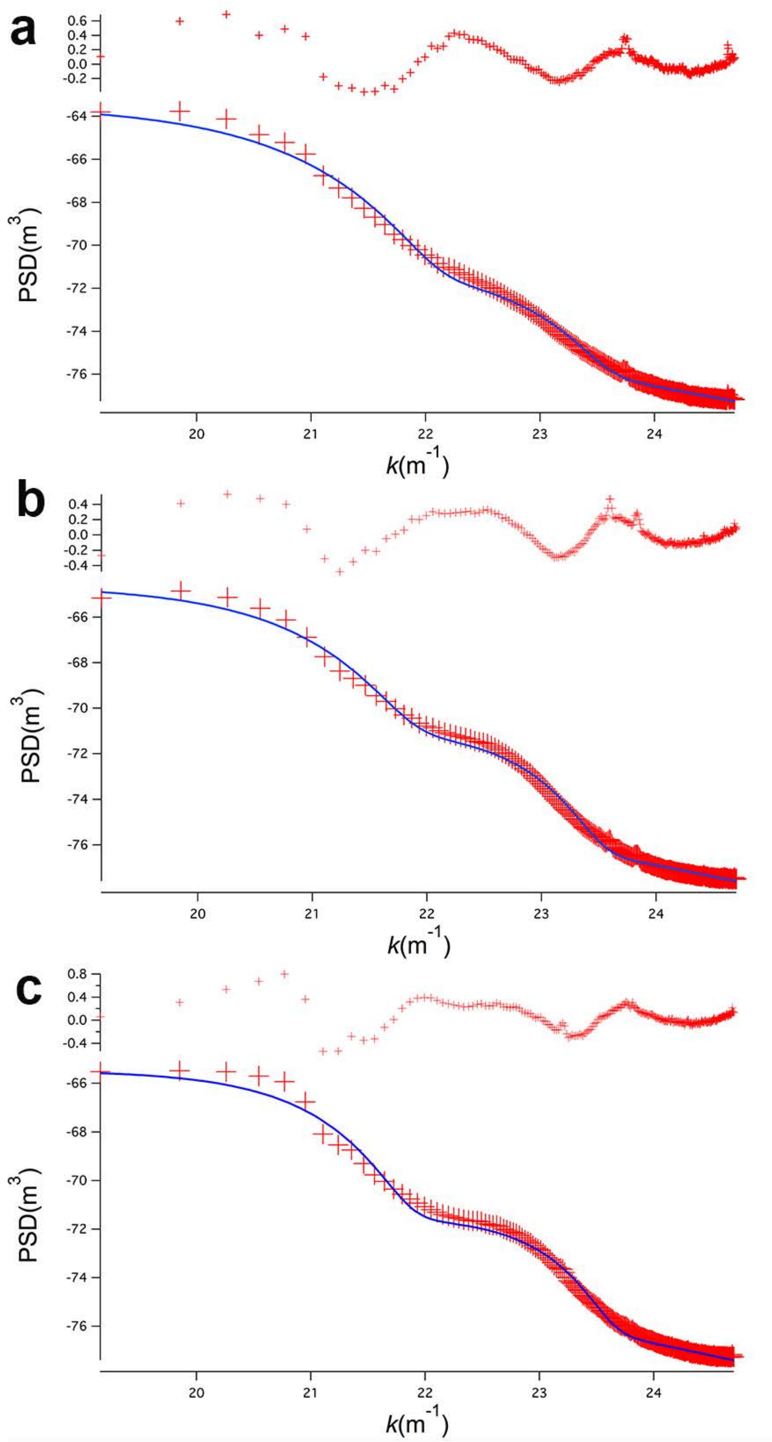

Figure S15. Average PSDs and their fittings displayed in full. (a) **NP2** in PO, (b) **NP2** in air, (c) **NP1** in air. In each graph, in the bottom plots the blue continuous line is the fit and the red crosses are experimental data, and the top plot is the fitting residuals. The plots in linear scale present the log of the PSD versus the log of *k.* These are the values that were fit in order to have errors of comparable fit throughout the plot.

Table S2. Fitting parameters for the average PSD curves present in Figure 2 of the main text.

File name	A1	Kc1	G1	A2	Kc2	G2	A3
NP1 in air	3.7e-29 ± 0	8.9015e+08 ± 7.04e+07	1.4847 ± 0.118	8.7e-32 ± 0	8.1749e+09 ± 2.24e+08	2.0693 ± 0.093	1.3e-23 ± 0
NP2 in air	8.8e-29 ± 0	5.9291e+08 ± 2.86e+07	1.1571 ± 0.0414	1.6e-31 ± 0	6.003e+09 ± 9.62e+07	1.7839 ± 0.0374	1.0659e-23 ± 1.42e-25
NP2 in PO	2.8e-28 ± 0	5.8605e+08	1.1635 ± 0	1.3e-31 ± 0	5.9239e+09 ± 1.1e+08	1.6124 ± 0.0372	1.5035e-23 ± 2.1e-25

Table S3. Summary of measurements for characteristic length scales of all samples.

	Operator 1		Operator 2		PSD fitting	
Sample	d(nm)	Std. Dev.	d(nm)	Std. Dev.	d(nm)	Conf. Int.
NP2 in air	0.83	0.18	0.94	0.16	1.04	0.016
NP2 in PO	0.80	0.16	0.92	0.13	1.06	0.019
NP1 in air	0.68	0.16	0.64	0.13	0.76	0.021

5. STM scan consistency by sum images

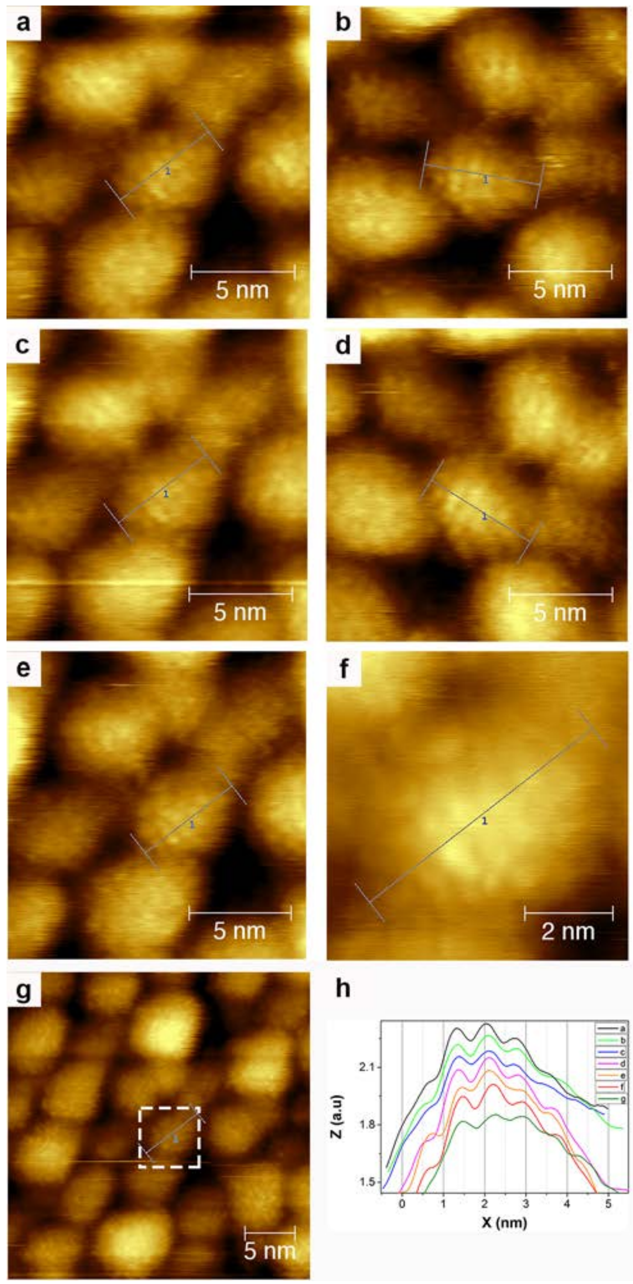

Figure SI6. Sums of STM topography trace and retrace scans of NP2 recorded in air at different scanning angles and scan sizes. (a) scanning angle = 0°, (b) 310°, (c) 0°, (d) 290°, (e,f,g) 0°.(h) Cross section lines going across the same particles show the remarkable consistency of the features on the NPs. The lines (marked by number 1) on each image (a-g) are the exact cross sections used and their ends indicate average width.

6. Image dataset for each STM scan

Imaging parameters for each image presented are given in the figure caption.

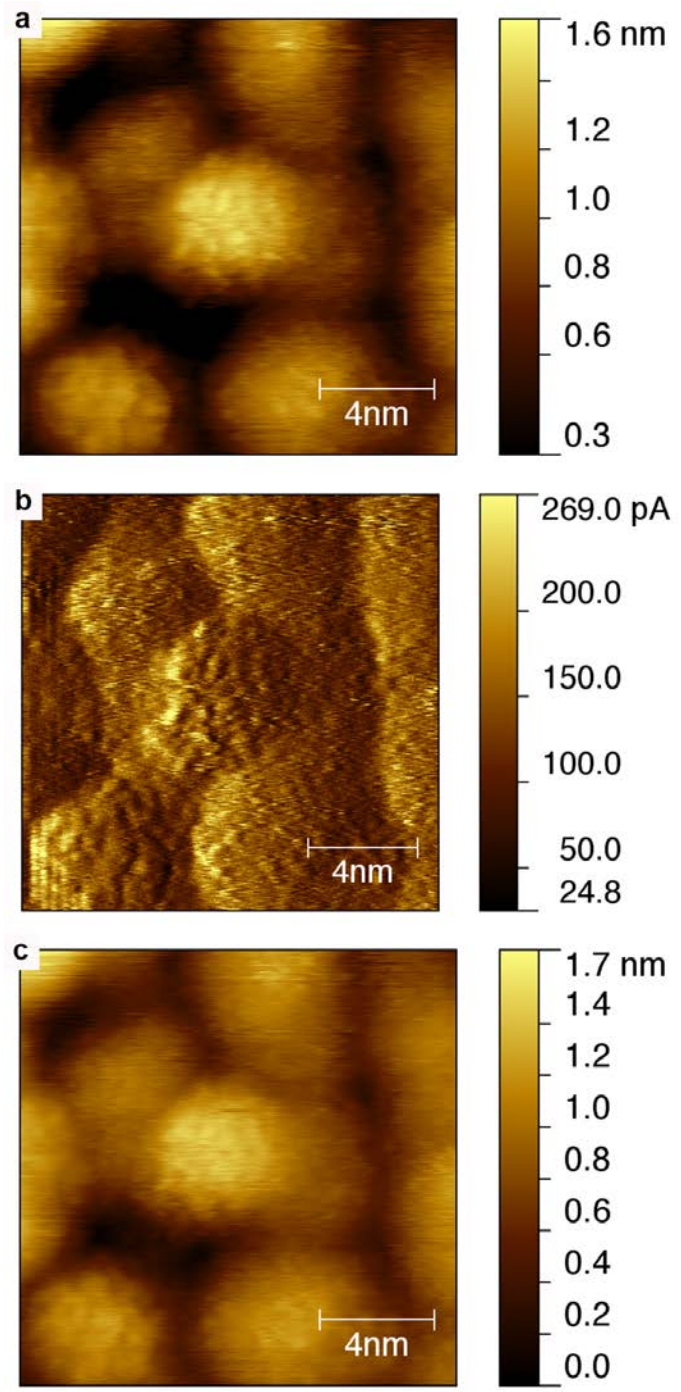

Figure S17. STM images of **NP2** in air. (a) topography trace image (b) current trace image (c) topography retrace image. Images recorded with Vb = +700 mV, It = 100 pA, Ss = 15x15 nm^2, Vt= 0.91 μm/s, Pi =0.42.

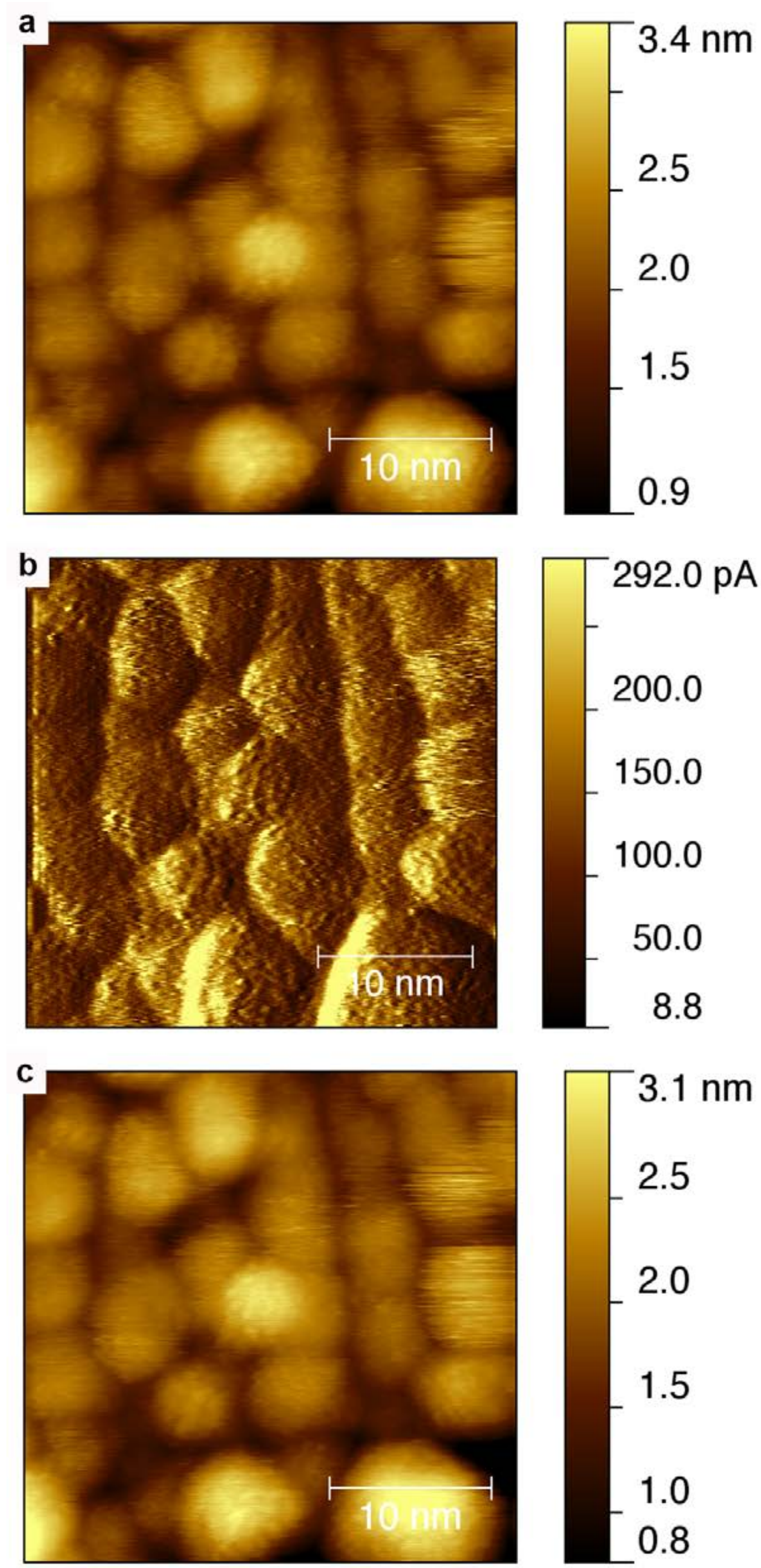

Figure S18. STM images of **NP2** in air. (a) topography trace image (b) current trace image (c) topography retrace image. Images recorded with Vb = +700 mV, It = 100 pA, Ss = 30x30 nm^2, Vt= 1.22 μm/s, Pi =0.42.

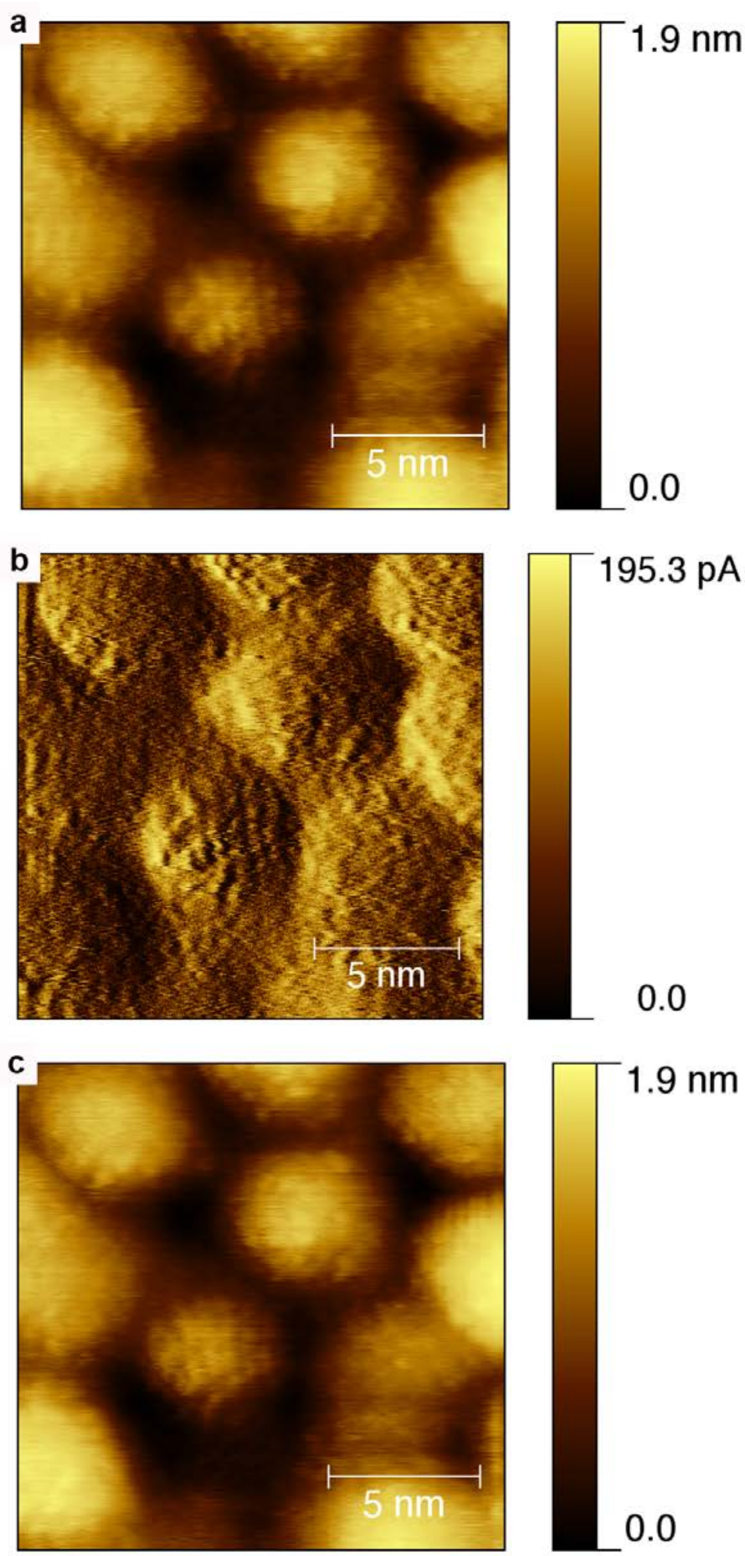

Figure S19. STM images of **NP1** in air. (a) topography trace image (b) current trace image (c) topography retrace image. Images recorded with Vb = +700 mV, It = 50 pA, Ss = 15.7x15.7 nm^2, Vt= 0.96 μm/s, Pi =0.45.

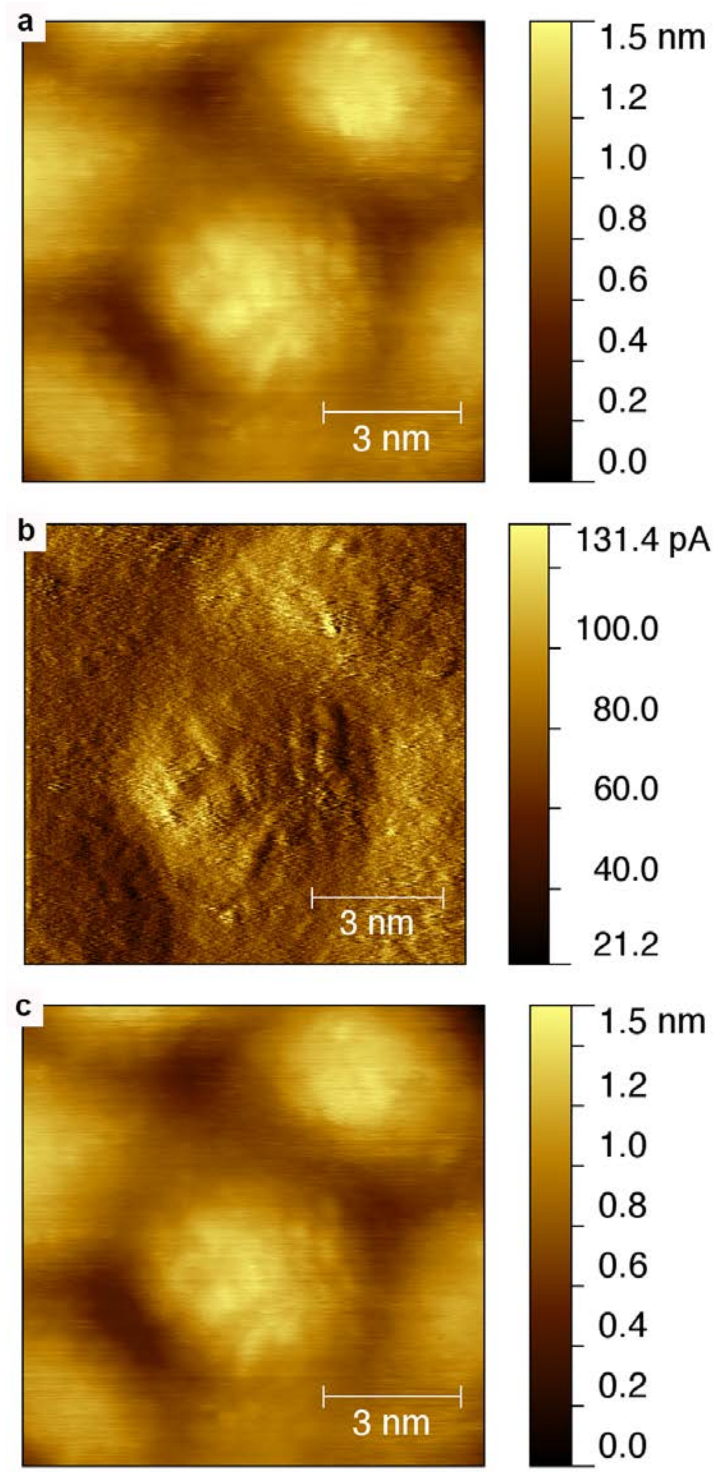

Figure S20. STM images of **NP1** in air. (a) topography trace image (b) current trace image (c) topography retrace image. Images recorded with Vb = +800 mV, It = 100 pA, Ss = 9.9x9.9 nm^2, Vt= 0.4 µm/s, Pi =0.45.

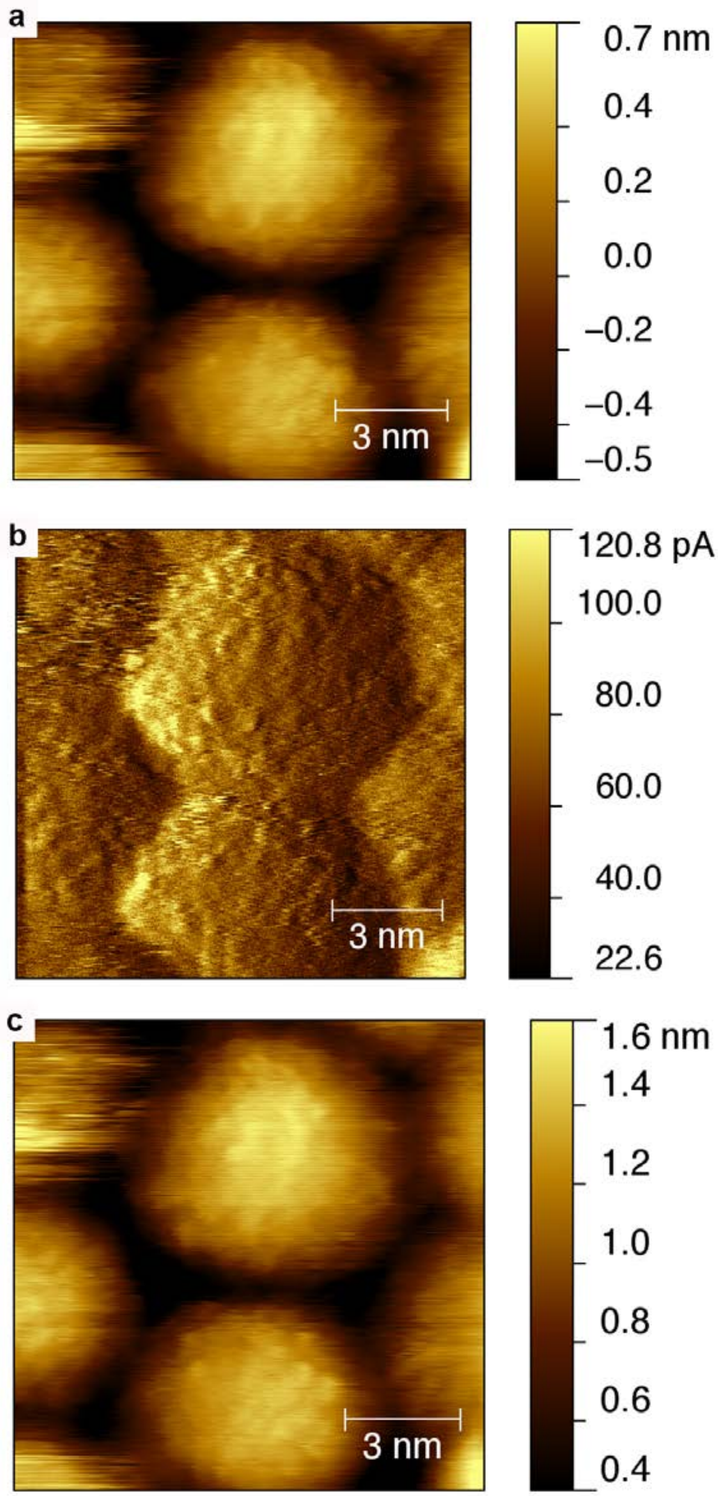

Figure S21. STM images of **NP2** in PO. (a) topography trace image (b) current trace image (c) topography retrace image. Images recorded with Vb = +500 mV, It = 50 pA, Ss = 12x12 nm^2, Vt= 0.73 µm/s, Pi =0.43.

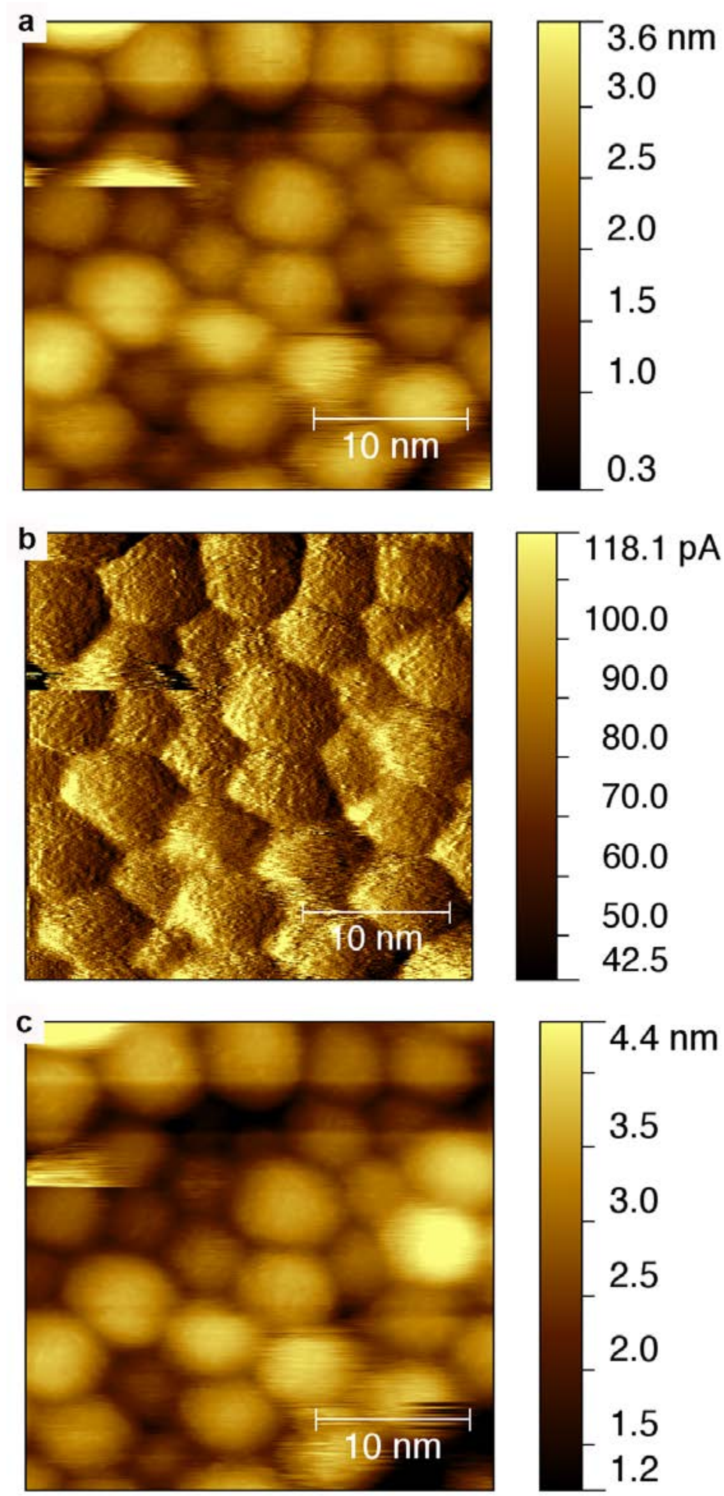

Figure S22. STM images of **NP2** in PO. (a) topography trace image (b) current trace image (c) topography retrace image. Images recorded with Vb = +500 mV, It = 50 pA, Ss = 30x30 nm^2, Vt= 0.73 μm/s, Pi =0.43.

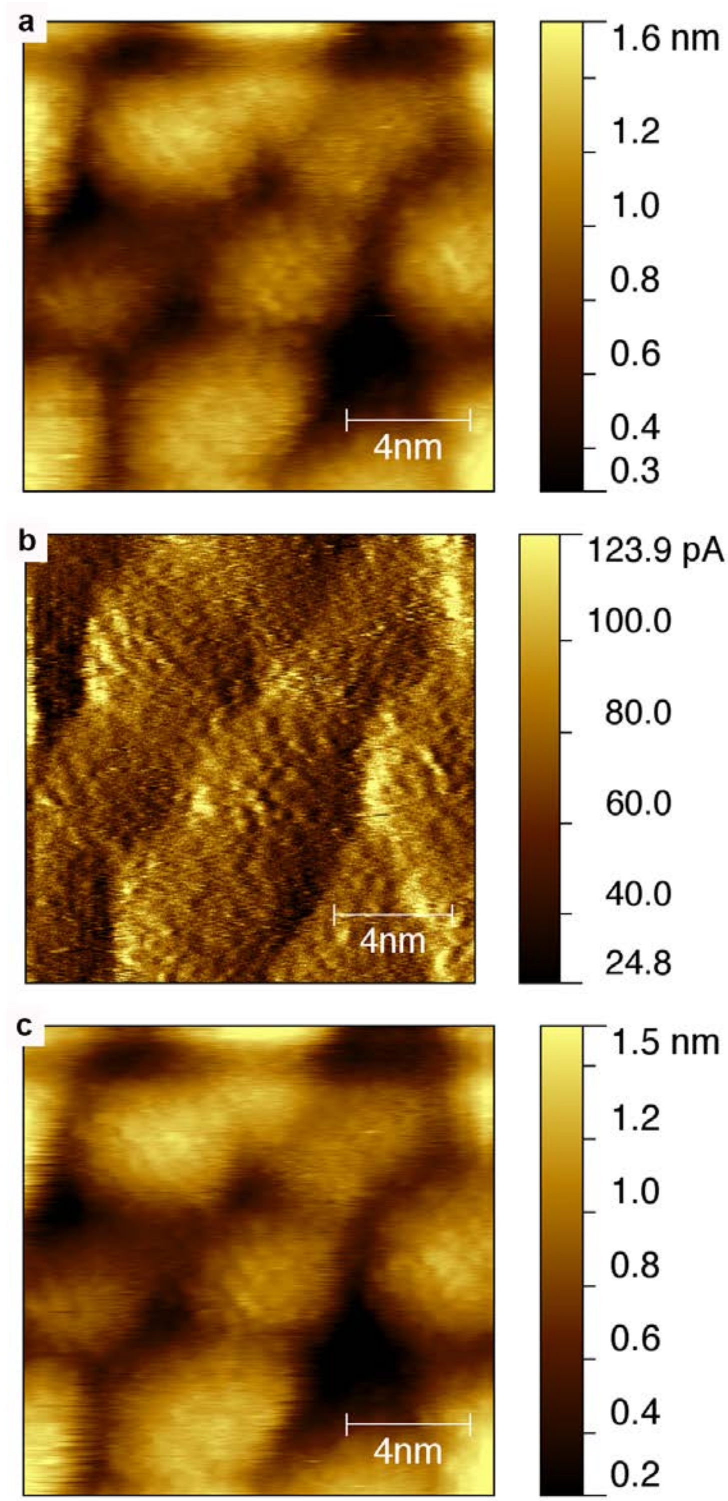

Figure S23. STM images of **NP2** in air. (a) topography trace image (b) current trace image (c) topography retrace image. Images recorded with Vb = +500 mV, It = 50 pA, Ss = 15x15 nm^2, Vt= 0.91 μm/s, Pi=0.41.

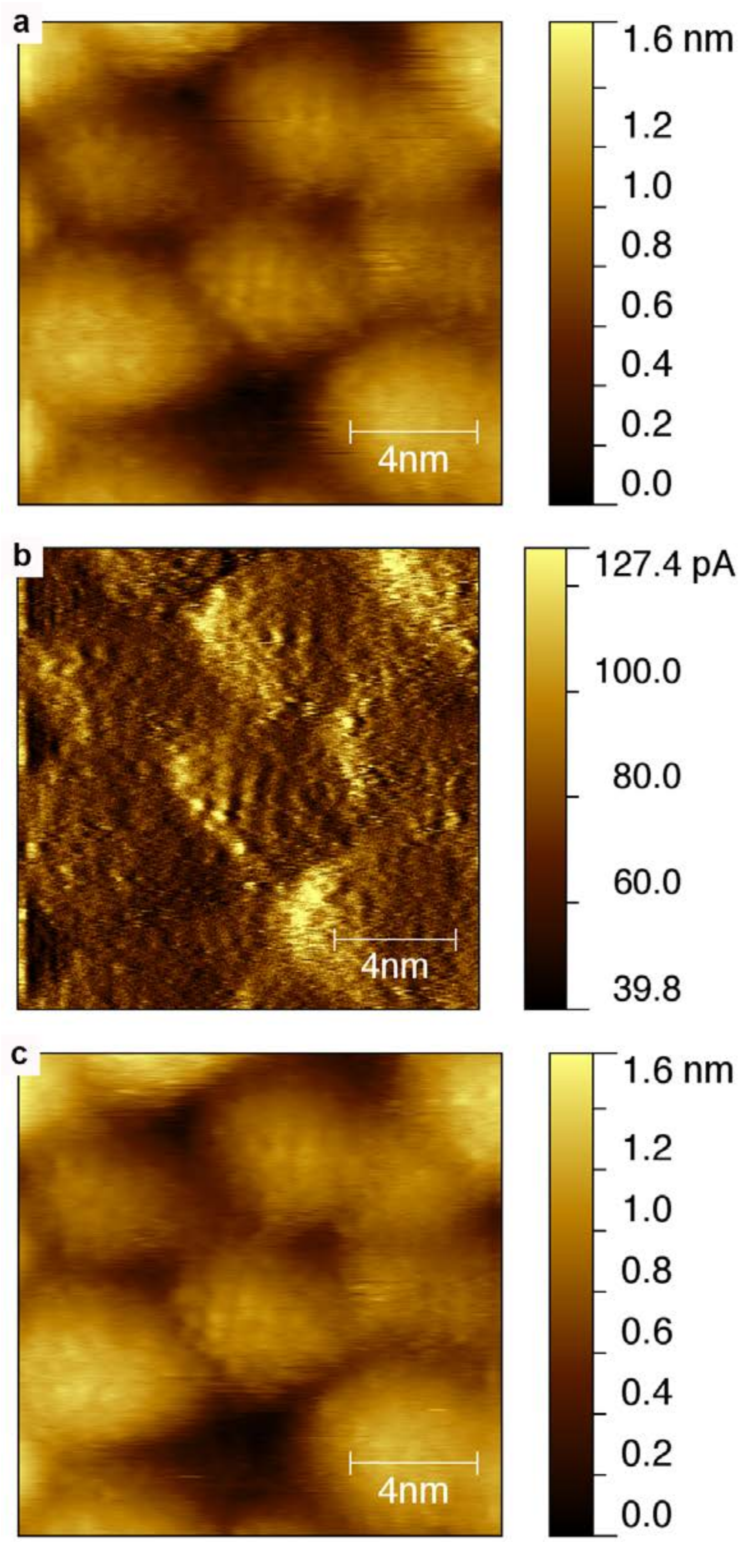

Figure S24. STM images of **NP2** in air. (a) topography trace image (b) current trace image (c) topography retrace image. Images recorded with Vb = +500 mV, It = 50 pA, Ss = 15x15 nm^2, Vt= 0.91 µm/s, Pi =0.41.

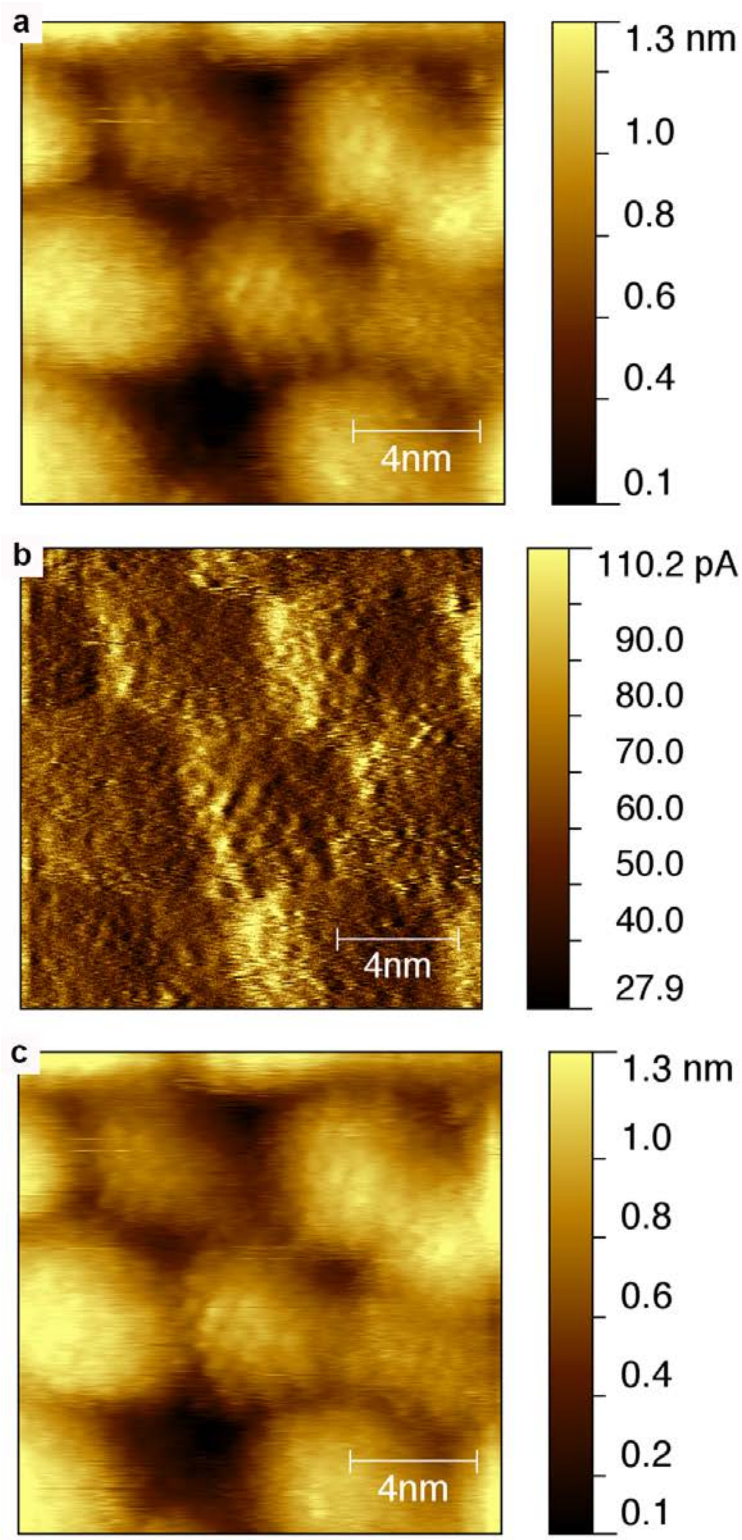

Figure S25. STM images of **NP2** in air. (a) topography trace image (b) current trace image (c) topography retrace image. Images recorded with Vb = +500 mV, It = 50 pA, Ss = 15x15 nm^2, Vt= 0.91 μm/s, Pi =0.41.

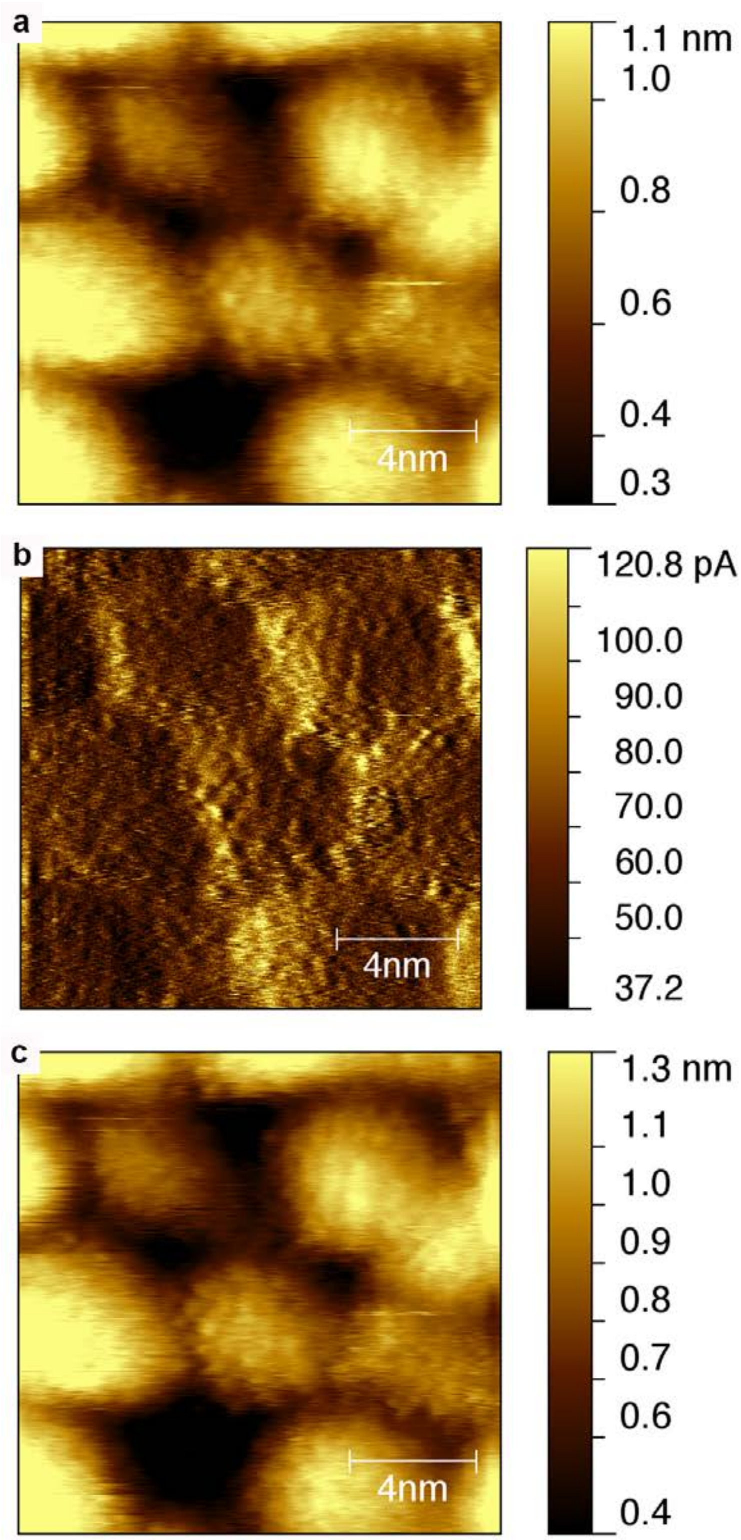

Figure S26. STM images of **NP2** in air. (a) topography trace image (b) current trace image (c) topography retrace image. Images recorded with Vb = +500 mV, It = 50 pA, Ss = 15x15 nm^2, Vt= 0.91 μm/s, Pi =0.41.

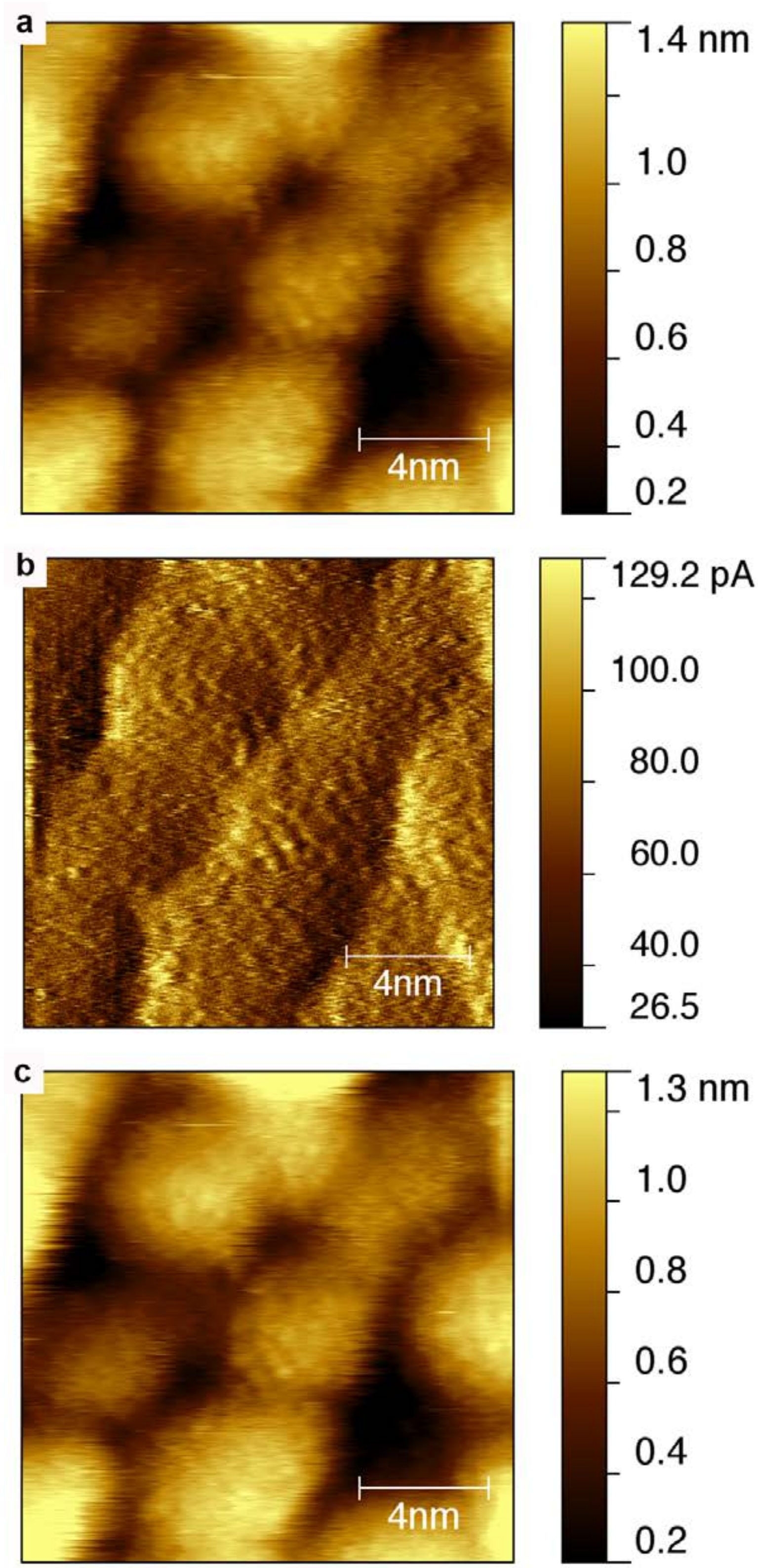

Figure S27. STM images of **NP2** in air. (a) topography trace image (b) current trace image (c) topography retrace image. Images recorded with Vb = +500 mV, It = 50 pA, Ss = 15x15 nm^2, Vt= 0.91 μm/s, Pi =0.41.

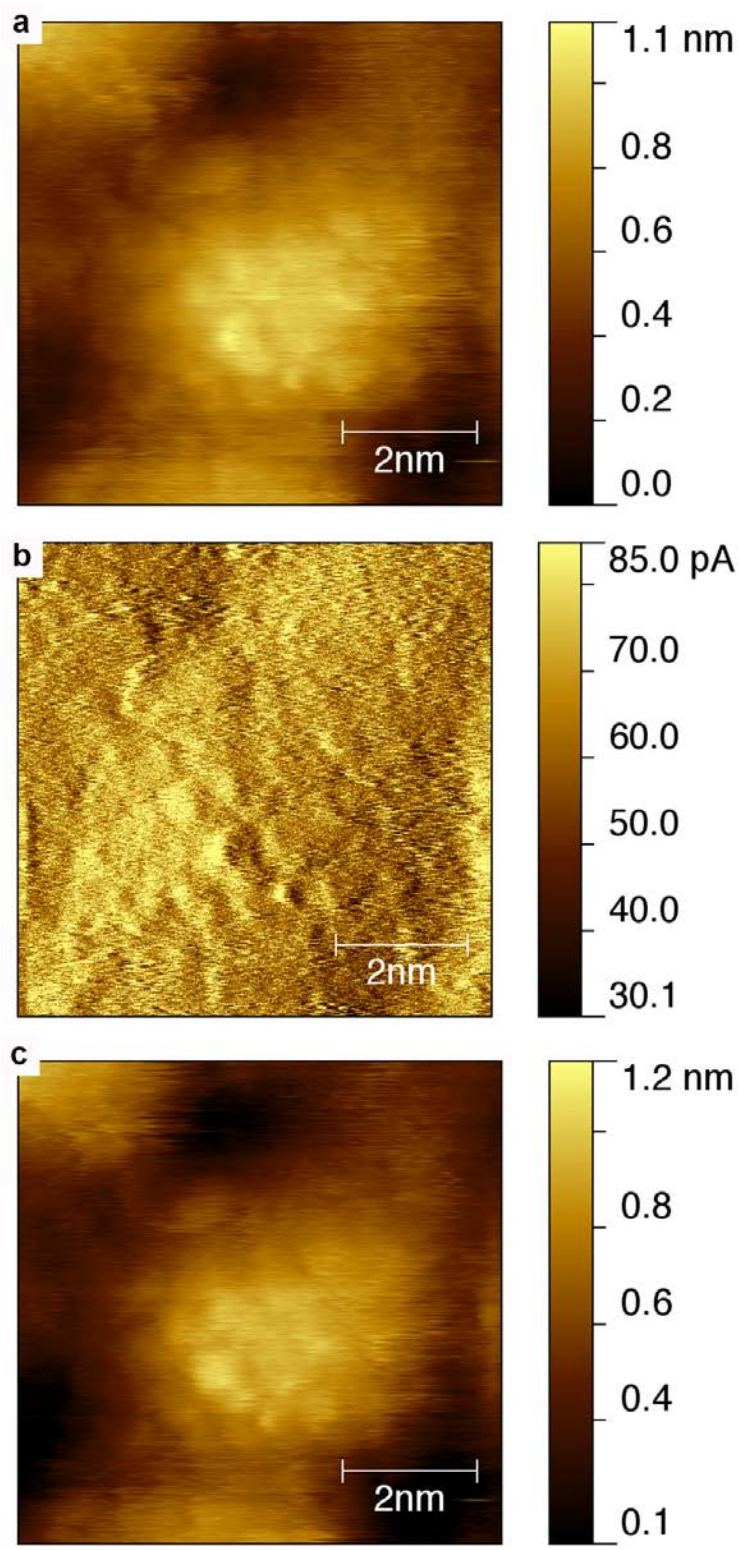

Figure S28. STM images of **NP2** in air. (a) topography trace image (b) current trace image (c) topography retrace image. Images recorded with Vb = +500 mV, It = 50 pA, Ss = 7x7 nm^2, Vt= 0.43 μm/s, Pi =0.41.

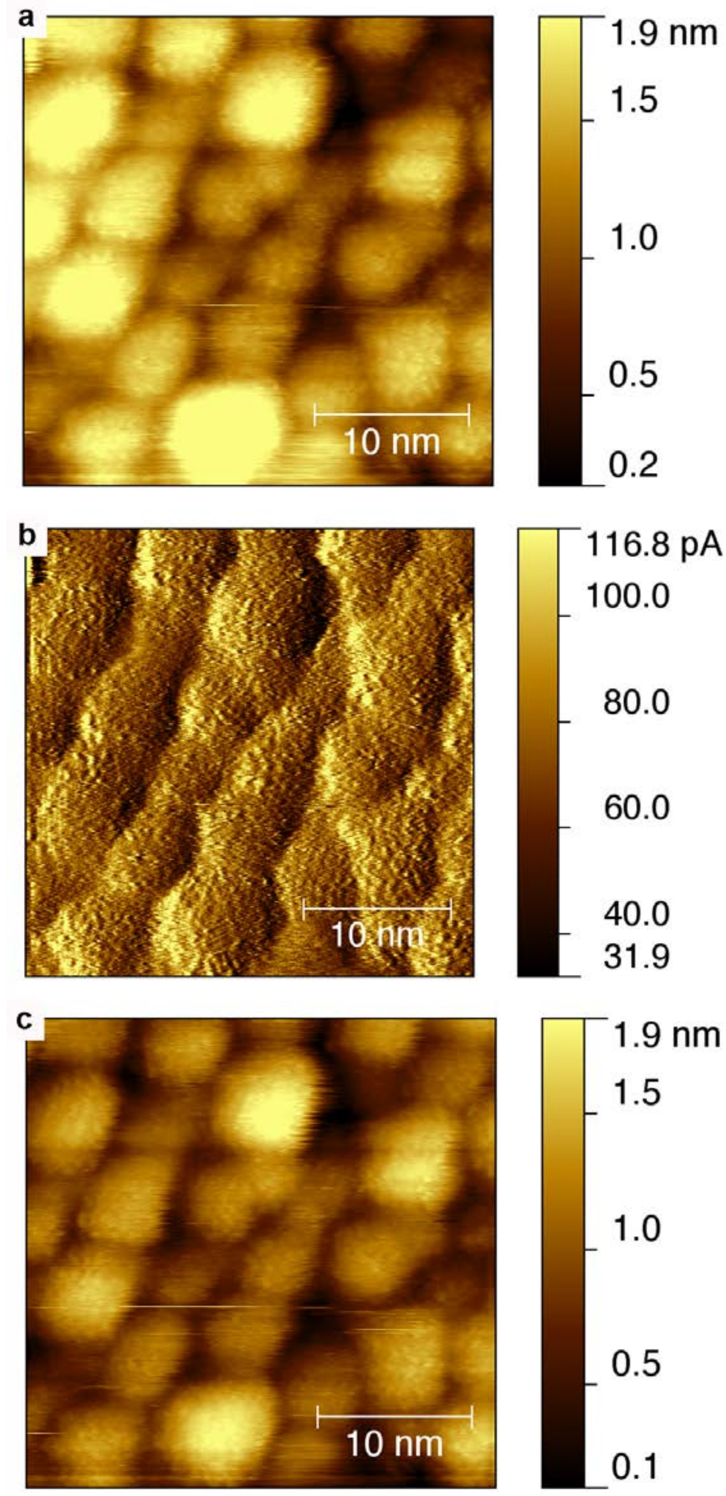

Figure S29. STM images of **NP2** in air. (a) topography trace image (b) current trace image (c) topography retrace image. Images recorded with Vb = +500 mV, It = 50 pA, Ss = 30x30 nm^2, Vt= 0.91 μm/s, Pi =0.41.

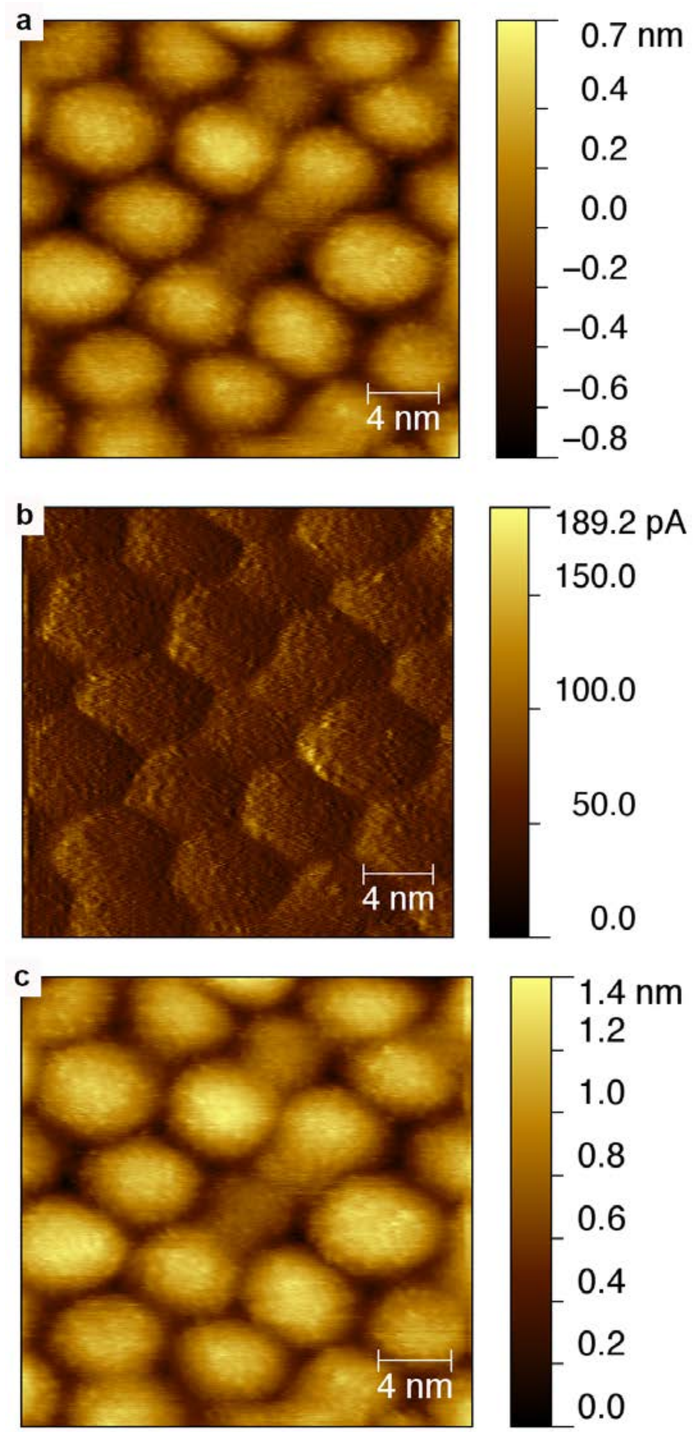

Figure S29. STM images of **NP1** in air. (a) topography trace image (b) current trace image (c) topography retrace image. Images recorded with Vb = +700 mV, It = 50 pA, Ss = 24x24 nm^2, Vt= 0.97 μm/s, Pi =0.48.

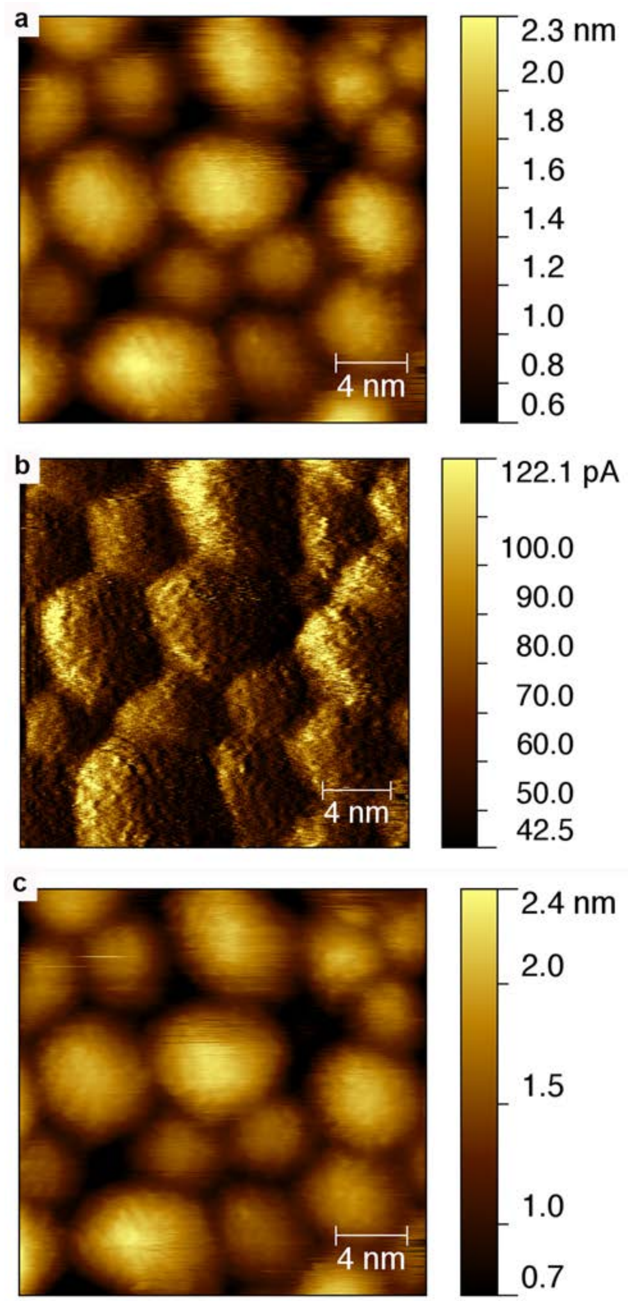

Figure S29. STM images of **NP2** in PO. (a) topography trace image (b) current trace image (c) topography retrace image. Images recorded with Vb = +500 mV, It = 50 pA, Ss = 23.3x23.3 nm^2, Vt= 0.9 μm/s, Pi =0.43.

---

1 D. Nečas and P. Klapetek, *Cent. Eur. J. Phys.*, 2012, **10**, 181.